



**HAL**  
open science

## Typology of planktonic food webs and associated emerging properties as indicators of the ecological status of a permanently disturbed Gulf of Gabès

Oumayma Chkili, Blanche Saint Béat, Kaouther Mejri Kousri, Marouan Meddeb, Paula Gauvin, Valerie David, Georges Safi, Asma Sakka Hlaili, Nathalie Niquil

### ► To cite this version:

Oumayma Chkili, Blanche Saint Béat, Kaouther Mejri Kousri, Marouan Meddeb, Paula Gauvin, et al.. Typology of planktonic food webs and associated emerging properties as indicators of the ecological status of a permanently disturbed Gulf of Gabès. *Journal of Marine Systems*, 2023, 242, pp.103948. 10.1016/j.jmarsys.2023.103948 . hal-04336431

**HAL Id: hal-04336431**

**<https://normandie-univ.hal.science/hal-04336431>**

Submitted on 11 Dec 2023

**HAL** is a multi-disciplinary open access archive for the deposit and dissemination of scientific research documents, whether they are published or not. The documents may come from teaching and research institutions in France or abroad, or from public or private research centers.

L'archive ouverte pluridisciplinaire **HAL**, est destinée au dépôt et à la diffusion de documents scientifiques de niveau recherche, publiés ou non, émanant des établissements d'enseignement et de recherche français ou étrangers, des laboratoires publics ou privés.

1 **Typology of planktonic food webs and associated emerging properties as**  
2 **indicators of the ecological status of a permanently disturbed Gulf of Gabès**

3 Oumayma Chkili<sup>1,2,3</sup>, Blanche Saint Béat<sup>4</sup>, Kaouther Mejri Kousri<sup>1</sup>, Marouan  
4 Meddeb<sup>1,2</sup>, Paula Gauvin<sup>5</sup>, Valerie David<sup>5</sup>, Georges Safi<sup>6</sup>, Asma Sakka Hlaili<sup>1,2</sup>,  
5 Nathalie Niquil<sup>3\*</sup>.

6

7 ✉ Nathalie Niquil  
8 [nathalie.niquil@unicaen.fr](mailto:nathalie.niquil@unicaen.fr)

9

10 <sup>1</sup> Université de Carthage, Faculté des Sciences de Bizerte, Laboratoire de Biologie Végétale et  
11 Phytoplanktonologie, Bizerte, Tunisie

12 <sup>2</sup> Université de Tunis El Manar, Faculté des Sciences de Tunis, Laboratoire des Sciences de  
13 l'Environnement, Biologie et Physiologie des Organismes Aquatiques LR18ES41, Tunis, Tunisie

14 <sup>3</sup> Université de Normandie, UNICAEN, UMR BOREA (MNHN, CNRS-8067, Sorbonne  
15 Universités, Université Caen Normandie, IRD-207, Université des Antilles), CS 14032, Caen,  
16 France

17 <sup>4</sup> Ifremer-Plouzané- DYNECO-PELAGOS, France

18 <sup>5</sup> Université de Bordeaux, UMR EPOC, CNRS, 5805, France

19 <sup>6</sup> France Energies Marines ITE-EMR, 525 Avenue Alexis de Rochon, 29280 Plouzané, France

20

21

22 Received 10 March 2023, Revised 9 October 2023, Accepted 20 November 2023, Available  
23 online 24 November 2023, Version of Record 29 November 2023.

24 Published in: Journal of Marine Systems

25 DOI: <https://doi.org/10.1016/j.jmarsys.2023.103948>

26 0924-7963/© 2023 Published by Elsevier B.V. All rights reserved.

27 **Link: <https://www.sciencedirect.com/science/article/abs/pii/S0924796323000921>**

28

29

30

31

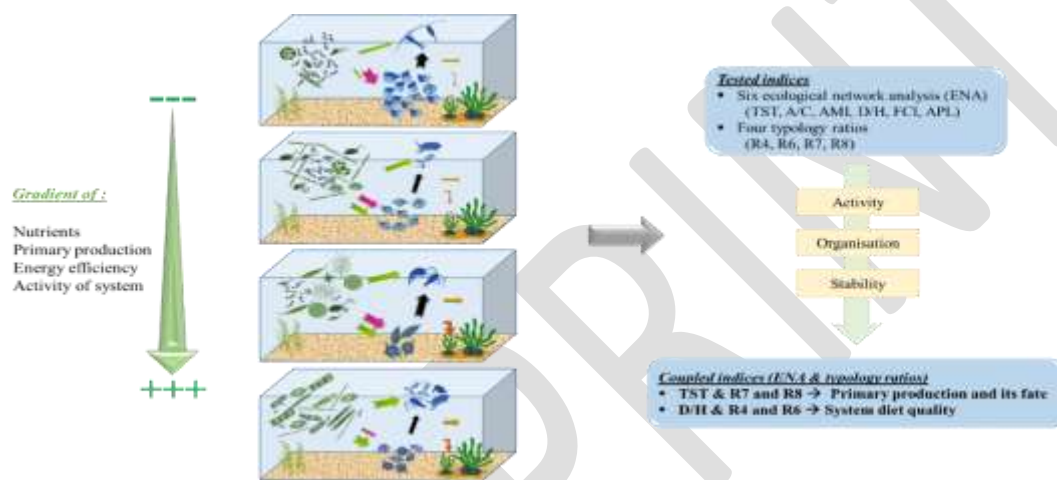
## 32 **Abstract**

33 This study highlights the importance of coupling the typology of planktonic food webs and their  
34 emerging properties to better describe the ecological status of an ecosystem under permanent  
35 disturbance mainly caused by phosphate industry. Linear inverse models were built to describe  
36 four stations under various levels of nutrient pressure, using the Markov Chain Monte Carlo  
37 method to estimate known and unknown carbon flows, later used to calculate food web  
38 typology ratios. Ecological network analysis (ENA) was used to describe the structural and  
39 functional properties of each food web. Based on the food web typology ratios, three planktonic  
40 trophic pathways (PTP) with different functional indices were distinguished according to  
41 nutrient stress. The microbial food web dominated in the least nutrient-rich environment. It  
42 mainly relied on phytoplankton production (picophytoplankton  $< 2 \mu\text{m}$ ) that was mainly  
43 transferred by the high microbivory of protozooplankton. In contrast, the herbivorous food web  
44 developed in the most nutrient-rich environment, where biogenic carbon was mainly produced  
45 by large phytoplankton (microphytoplankton  $> 10 \mu\text{m}$ ) and channeled to higher trophic levels  
46 by herbivorous protozooplankton and metazooplankton. In the other two stations – moderately  
47 nutrient-rich systems – the PTP acted as a multivorous food web. Phytoplankton (small and  
48 large size fractions) and non-living components (detritus and dissolved organic carbon) played  
49 a significant role in carbon production, and competed with protozooplankton and  
50 metazooplankton for its transport. ENA indices revealed that the herbivorous food web, with  
51 the highest total system throughput and lowest relative Ascendency and cycling, was the most  
52 active but the least organized and stable system. In contrast, the microbial food web, with the  
53 lowest total system flux and highest Ascendency, was least active but more organized than the  
54 herbivorous food web. The multivorous food web displayed the most recycling and most  
55 organized system, with high values of the detritivory-to-herbivory ratio, cycling and  
56 Ascendency. In addition to ENA indices, which are considered effective tools for studying the  
57 structural and functional properties of food webs, marine ecosystem management efforts

58 heavily focus on using the "marine food web" as a descriptor of the system's ecological status.  
59 However, we suggest that the combination of food web typology and ecological indices could  
60 be used as an effective tool for the management and assessment of ecosystem health wherever  
61 possible, as well as for the study of anthropogenic pressures.

62 **Keywords:** Food-web modeling, ecological network analysis, typology ratios, Mediterranean  
63 coastal ecosystem, anthropogenic pressure.

## 64 Graphical abstract



65

## 66 Highlights

- 67 • Food web typology ratios and ENA indices were used to describe the structural and  
68 functional properties of three food webs quantified along a gradient of nutrient stress.
- 69 • In the most nutrient-rich waters, the herbivorous food web was most active but least  
70 organized and stable.
- 71 • In the nutrient-poorest waters, the microbial food web was least active but more  
72 organized than the herbivorous one.
- 73 • In the intermediate-nutrient-level waters, the multivorous food web was the most  
74 recycled and organized system.
- 75 • Food web typology ratios + ecological ENA indices represent an effective tool for  
76 managing and assessing ecosystem health.

## 77 **1. Introduction**

78 In marine waters, primary production can reach higher consumers through different types  
79 of food webs. The size structure of phytoplankton is the most relevant functional trait driving  
80 carbon transfer pathways. Small phytoplankton are mainly involved in microbial food webs,  
81 dominated by protozooplankton (PRO) grazing, while large phytoplankton are mainly  
82 consumed by metazooplankton (MET) (e.g., copepods) leading to herbivorous food webs. In-  
83 between these two contrasting food webs, the trophic continuum includes multivorous  
84 pathways in which microbial and herbivorous trophic patterns both play significant roles  
85 (Legendre and Rassoulzadegan, 1995, 1996). These food webs channel biogenic carbon to  
86 higher consumers with different efficiencies. Consequently, changes in the size structure of  
87 phytoplankton in response to any environmental variation leads to a shift in the food web  
88 structure that ultimately influences the ability of the ecosystem to export or recycle biogenic  
89 carbon (Decembrini et al., 2009; Legendre and Le Fèvre, 1989; Meddeb et al., 2019).

90 Determining marine food web types is of great ecological and practical interest, since it  
91 is the main step toward characterizing ecosystem functioning and understanding the flows of  
92 material and energy within marine planktonic communities. For example, in the fisheries sector,  
93 identifying the type of food web can provide a clear idea of the capacity of the system to support  
94 the fishing activity, and this helps for proper exploitation and management (Hill et al., 2006;  
95 Gaichas, 2008; Knights et al., 2013; Subramaniam et al., 2022). In ecosystems subject to natural  
96 and anthropogenic disturbances, knowledge of the marine food web is an essential step in  
97 assessing ecosystem responses to these disturbances (Gotwals and Songer, 2010; Lewis et al.,  
98 2022). Environmental managers who ignore the structure and functioning of food webs face the  
99 danger of making choices that might ultimately result in even greater costs. Impacts may  
100 include a health decline of the ecosystem, resulting in less services provided and higher  
101 expenses for restoration and repair. Food webs are currently in the foreground in marine  
102 ecosystem management programs. The European Marine Strategy Framework Directive has

103 retained the “marine food web” as a descriptor of the ecological status of the system (Cardoso  
104 et al., 2010; European Commission, 2010). This means that one of the major criteria for "good  
105 environmental status" is based on the typology of food webs, highlighting the usefulness of  
106 identifying the structure and functioning of food webs for managing marine ecosystems.

107 Several modeling approaches have been developed to characterize marine food webs.  
108 These models can provide ecological underpinnings for ecosystem services and the  
109 management of natural marine systems (Carpenter et al., 2009; Bagstad et al., 2013; Beske-  
110 Janssen et al., 2015). Ecopath with Ecosim (EwE) food web modeling is an approach mainly  
111 used to study upper trophic levels subject to fishing (Pauly et al., 2000; Christensen et al., 2005;  
112 Sreekanth et al., 2021) and to assess the impact of human exploitation and environmental  
113 changes on aquatic food webs (Steenbeek et al., 2018). The linear inverse model (LIM), as  
114 defined by Vézina and Piatt (1988), is derived from the physical sciences and is considered  
115 among the most useful methods in the study of the state of marine ecosystems (Niquil et al.,  
116 2011; Pacella et al., 2013; Taffi et al., 2015; Hines et al., 2018). This method has been combined  
117 with the Markov Chain Monte Carlo (MCMC) technique to become the innovative LIM  
118 Markov Chain Monte Carlo (LIM-MCMC; Meersche et al., 2009). LIM-MCMC estimates  
119 uncertainty in flows and indices of structural and functional properties of the food web (De  
120 Laender et al., 2010; Grami et al., 2011; Niquil et al., 2011; Saint-Béat et al., 2013; Chaalali et  
121 al., 2015; Hines et al., 2018).

122 Food web determination and modeling requires knowledge of carbon flows, which cannot  
123 always be measured in the field. Therefore, several researchers have provided operational  
124 criteria to identify and describe food web types, based on ratios calculated from carbon stocks  
125 or fluxes easy to estimate in the field (Legendre and Rassoulzadegan, 1995; Mousseau et al.,  
126 2001; Sakka Hlaili et al., 2014). Based on a list of numerous LIM models of plankton food  
127 webs, Sakka Hlaili et al. (2014) proposed seven food web typology ratios, which can be used  
128 as indicators of the type of trophic pathways in natural planktonic systems.

129 Food web modeling is often coupled with ecological network analysis (ENA). ENA  
130 provides ecological indicators that characterize ecosystem functioning in terms of activity,  
131 retention capacity, organization and food web maturity (Ulanowicz, 1986; Christensen, 1995;  
132 Christian et al., 2009; Bodini et al., 2012a; Pezy et al., 2017; de Jonge and Schückel, 2021).  
133 ENA indicators are frequently used to assess the impact of natural and anthropogenic pressures  
134 on coastal marine ecosystems (Belgrano et al., 2005; Niquil et al., 2014a; Piroddi et al., 2015;  
135 Chaalali et al., 2016). They also provide useful information on the degree of stress and stability  
136 of food webs (Grami et al., 2008; Heymans et al., 2014; Saint-Béat et al., 2015). In addition,  
137 recent studies have presented a set of ENA indices that are most appropriate for studying the  
138 health status of ecosystems and could be applied by ecosystem managers (Fath et al., 2019a;  
139 Safi et al., 2019). ENA indices were recently applied in the context of the assessment of the  
140 quality of four marine ecosystems in the Oslo-Paris (OSPAR) Quality Status Report 2023  
141 (Schückel et al., 2022). The report showed that ENA indices could be used to support the  
142 assessment of the structure and functioning of food webs.

143 Although much effort has been undertaken to assess the ecological state of Mediterranean  
144 ecosystems (Méndez et al., 2008; Liqueste et al., 2016; Meddeb et al., 2019; Danovaro et al.,  
145 2020; Decembrini et al., 2021), studies on the food web structure and function and on ecosystem  
146 health remain scarce. For example, MerMex group reported that common indicators of  
147 ecological degradation of Mediterranean marine ecosystems are biomass depletion at high  
148 trophic levels, simplification of food webs, and shifts in biomass and productivity to lower  
149 trophic levels (Durrieu de Madron et al., 2011). Meddeb et al. (2018) showed that LIM-MCMC  
150 food web models combined with ENA indicators are a powerful approach to detect changes in  
151 the environmental status and anthropogenic impacts in southwestern Mediterranean  
152 ecosystems. Several Mediterranean ecosystems, particularly coastal waters, are under strong  
153 anthropogenic pressure that causes an imbalance in their communities and biodiversity, with a  
154 serious threat on their ecosystem services (Templado, 2014; Danovaro, 2003; Bevilacqua et al.,  
155 2021). Therefore, predicting the consequences of anthropogenic disturbances on ecosystem



156 functioning by a holistic approach is very relevant. The present study aims to investigate the  
157 structure of the trophic food web and its emerging properties in a Mediterranean site under  
158 permanent anthropogenic pressure (the Gulf of Gabès). It also aims to provide useful ecological  
159 indicators for assessing the health status of the ecosystem, to be considered by environmental  
160 managers. The Gulf is highly impacted by the Tunisian Chemical Group (TCG), which  
161 discharges high quantities of phosphogypsum into the sea that bring high inputs of nutrients  
162 and metals and lead to chronic disruption of the ecosystem (Ayadi et al., 2015; El Zrelli et al.,  
163 2015). Our previous study in the Gulf (Chkili et al., 2023) was conducted in four stations located  
164 at different distances from the TCG complex (Fig. 1). It showed a spatial nutrient gradient  
165 causing significant spatial variations in the size structure and production of phytoplankton. This  
166 was determined with a spatial change in the community composition of PRO and MET,  
167 zooplankton grazing and particle sinking.

168 In this paper, we used the planktonic carbon stock and flux data determined in our  
169 previous study (Chkili et al., 2023), and measured dissolved organic carbon (DOC) and  
170 particulate organic carbon (POC) stocks. Then, the LIM-MCMC approach was applied to  
171 characterize planktonic food webs and find out what this implied in terms of overall changes in  
172 the food web. We used models calculated from LIM-MCMC to explore the planktonic  
173 community, highlighting the role played by nutrients in determining phytoplankton size  
174 structure. This overview of the planktonic food web allowed us to test the performance of  
175 indices commonly used in food web theory to identify the most appropriate ones for practical  
176 management. We used a multivariate analysis to achieve a correlative approach of nutrient  
177 gradients and indicators of proposed planktonic food web functioning by combining two types  
178 of functional indicators: ENAs that apply to all food webs (Niquil et al., 2012; Meddeb et al.,  
179 2018; 2019), and  $R_n$  ratios that distinguish planktonic food web types (Sakka Hlaili et al., 2014).  
180 Our objective was to provide useful and user-friendly indicators for specialists and non-  
181 specialists alike.

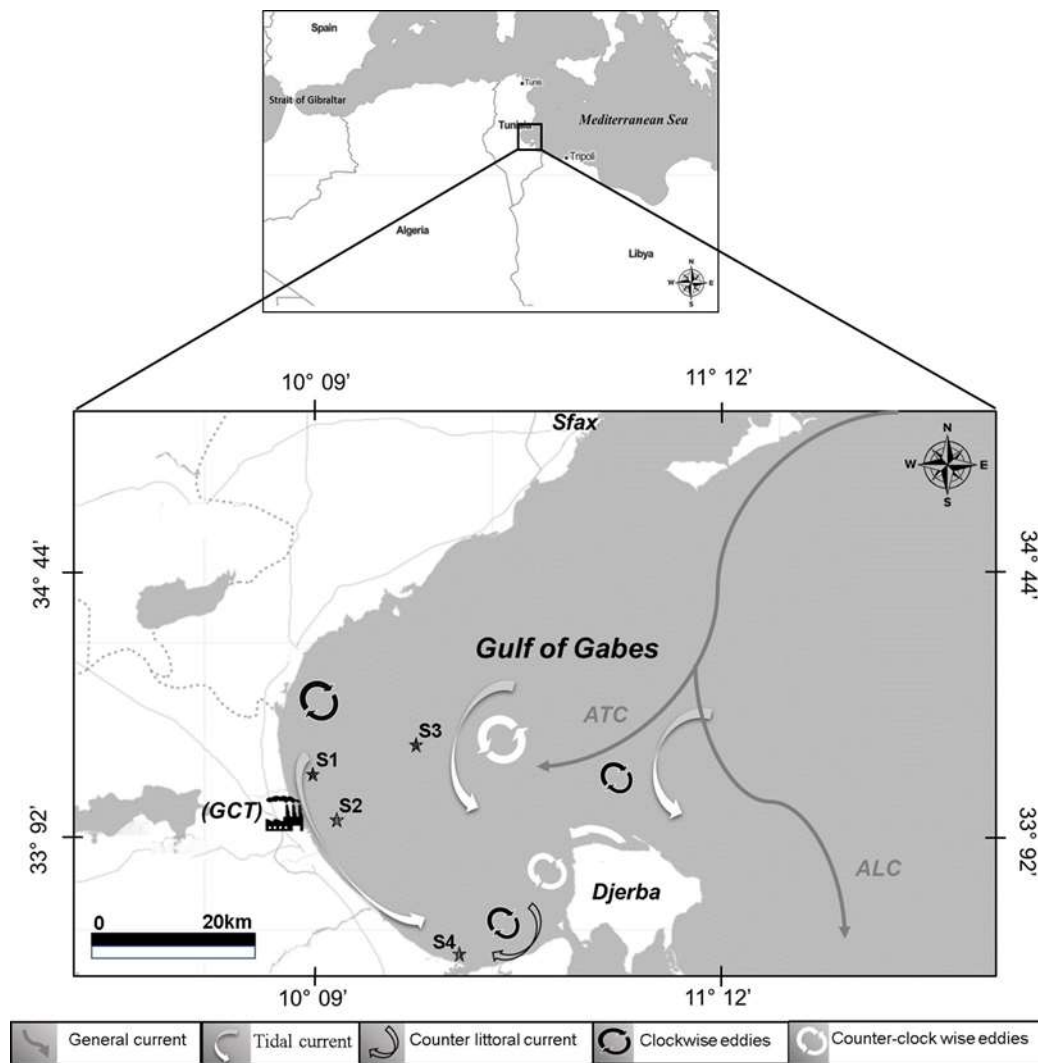


## 182 **2. Materials and Methods**

### 183 **2.1. Study Site**

184 The Gulf of Gabès is located on the south-eastern coast of Tunisia (Fig. 1). It represents more  
185 than half of the Tunisian coastline with about 700 km and has the largest continental shelf in the  
186 Mediterranean Sea. Its outline measured only on the 20-metre isobath is 110 nautical miles. The 50-  
187 metre depth extends to more than 70 nautical miles off Kerkennah Islands (Hattour et al., 2010).  
188 The Gulf is characterized by a complex water circulation resulting from the combination of general  
189 currents, tidal currents, wind-driven currents and/or swell or littoral currents, and tides reach the  
190 highest range in the Mediterranean sea (~ 2 m) (Hattour et al., 2010; Othmani et al., 2017). The Gulf  
191 hosts nutrient-rich waters as a result of inputs from anthropogenic activities (Bel Hassen et al., 2009;  
192 Drira et al., 2009; Khammeri et al., 2018), in contrast with the well-known oligotrophy of the  
193 Eastern Mediterranean Basin (D'Ortenzio and Ribera d'Alcalà, 2009; Ben Brahim et al., 2010). The  
194 Gulf is a highly productive ecosystem supporting a high marine biodiversity and contributing up to  
195 ~50% of the national fish production (DGPA 2015; Béjaoui et al., 2019). It also constitutes a crucial  
196 nursery ecosystem for the Mediterranean sea (Enajjar et al., 2015; Koched et al., 2015). This  
197 ecosystem was recently considered as one out of eleven consensus eco-regions in the Mediterranean  
198 Sea and is classified as a shallow-water region characterized by phytoplankton blooms (Ayata et al.,  
199 2018). Nevertheless, the Gulf is identified as a hotspot of anthropogenic pressures (Reygondeau et  
200 al., 2017) because it is strongly impacted by industrialization, notably discharges from phosphate  
201 production plants, mainly the TCG (Boudaya et al., 2019; Kmiha-Megdiche et al., 2021).  
202 Overfishing is also an increasing problem in the Gulf, leading to an imbalance of the ecosystem and  
203 the decline of fisheries resources (Béjaoui et al., 2019).

204



205

206

207 **Fig .1.** Location of the sampling stations and hydrodynamic circulation in the Gulf of Gabès,  
208 southeastern Mediterranean Sea. (From [Chkili et al., 2023](#))

## 209 2.2. Sampling and water analyses

210 Sampling was conducted in the fall of 2017 at four stations selected on either side of the main  
211 source of contamination (TCG) ([Fig. 1](#)). Station S2 was located in front of the phosphoric acid  
212 facility and was suspected to be most affected by phosphogypsum loading; stations S1 and S4 were  
213 also located in the marine coastal zone, north and south of S2, respectively, and S3 was an offshore  
214 station in front of S1. [Chkili et al. \(2023\)](#) showed that anthropogenic nutrient loading coupled with  
215 the complex hydrodynamic circulation within the Gulf create north-south (from S1 to S4) and coast-  
216 offshore (from S1 to S3) ascending gradients of nutrients.

217 Water was collected at three depths at each station (between 0.5 and 14 m depending on the  
218 maximum water depth of the station) using an acid-washed water sampler (HydroBios). Subsamples

219 (5 mL) were immediately filtered on sterilized 0.2- $\mu\text{m}$  polycarbonate filters and frozen in acid-  
220 washed vials at  $-20\text{ }^{\circ}\text{C}$  until DOC analysis using a Shimadzu TOC-5000A autoanalyser (Sharp et  
221 al., 1993). The remaining water was pre-filtered through a 200- $\mu\text{m}$  mesh screen to remove MET,  
222 and several subsamples were taken to analyze nutrients, POC, bacterioplankton (BAC), size-  
223 fractioned phytoplankton (picophytoplankton, PIC:  $< 2\text{ }\mu\text{m}$ ; nanophytoplankton, NAN: 2-10  $\mu\text{m}$ ;  
224 microphytoplankton, MIC: 10-200  $\mu\text{m}$ ) and protozooplankton (PRO). Most of these analyses are  
225 described in Chkili et al. (2023). Briefly, inorganic nutrients ( $\text{N}_{\text{inorg}}$ :  $\text{NO}_2^- + \text{NO}_3^- + \text{NH}_4^+$ ;  $\text{P}_{\text{inorg}}$ :  
226  $\text{PO}_4^{3-}$ ;  $\text{Si}(\text{OH})_4$ ) and organic nitrogen ( $\text{N}_{\text{org}}$ ) and phosphorus ( $\text{P}_{\text{org}}$ ) were measured using a BRAN  
227 & LUEBBE type 3 autoanalyzer (Bran + Luebbe Co., Germany). Subsamples for POC  
228 determination were filtered on pre-combusted ( $450\text{ }^{\circ}\text{C}$ , 24 h) GF/F filters (21 mm) and analyzed by  
229 the high combustion method and mass spectrometry (Raimbault et al., 2008). The subsamples were  
230 fixed with 20% paraformaldehyde solution, placed at  $4\text{ }^{\circ}\text{C}$  in the dark for 15 min, and finally frozen  
231 at  $-80\text{ }^{\circ}\text{C}$  in liquid nitrogen until analysis with a CyFlow® Space flow cytometer (Partec) to  
232 determine BAC and PIC abundances, according to Khammeri et al. (2020, 2018). The samples for  
233 NAN and MIC analyses were fixed with acid Lugol solution (4% final concentration), while the  
234 samples for PRO analysis were fixed with alkaline Lugol solution at 5% final concentration (Parsons  
235 et al., 1984; Sherr and Sherr, 1993). The cell abundances and species compositions of these  
236 planktonic groups were determined under an inverted microscope (Motic AE31E, 100 $\times$ objective)  
237 (Utermöhl, 1931). To determine MET abundance and composition, a WP2 200- $\mu\text{m}$  mesh net, with  
238 ring diameter of 28 cm, was used. The net was pulled vertically at a speed of  $1\text{ m s}^{-1}$  from depths  
239 10m at S1, 11m at S2 and S4 and 12m at S3 to the surface. A flow meter was used to determine the  
240 volume of water filtered during the towing of the net.

### 241 **2.3. Plankton data**

242 Data about planktonic carbon stocks and carbon fluxes were sourced from Chkili et al. (2023).  
243 Biovolumes of BAC, PIC, NAN, MIC and PRO were converted into carbon contents using specific  
244 conversion factors or formulae (Table 1 in Meddeb et al., 2018). The length and width of MET

245 organisms were measured and converted to carbon contents using conversion factors or formulae  
246 corresponding to each taxonomic group (Table 1 in Meddeb et al., 2018). The cell carbon of each  
247 plankton community was multiplied by its abundance to get its carbon concentration. DOC  
248 concentrations were obtained considering that 1  $\mu\text{M}$  of DOC was equal to 12  $\text{mg C m}^{-3}$  (Grami et  
249 al., 2008). Detrital organic carbon (DET) was estimated as POC minus the carbon biomasses of all  
250 organisms. Finally, for each planktonic compartment, carbon concentrations ( $\text{mg C m}^{-3}$ ) from the  
251 three depths were vertically integrated over the maximum depth of each station to get carbon stocks  
252 ( $\text{mg C m}^{-2}$ ).

253 Production rates ( $\text{mg C m}^{-2} \text{d}^{-1}$ ) of BAC and size-fractionated phytoplankton (PIC, NAN and  
254 MIC) as well as their grazing rates by PRO ( $\text{mg C m}^{-2} \text{d}^{-1}$ ) were estimated using the dilution  
255 technique (Landry and Hassett, 1982; Dokulil and Qian, 2021). The experimental procedure, the  
256 analysis and the rate estimation are detailed in Chkili et al. (2023). The relative contribution of PIC,  
257 NAN and MIC to primary production was calculated as the production rate of each size fraction  
258 divided by the total phytoplankton production rate multiplied by 100.

259 Grazing of phytoplankton (NAN and MIC) by MET ( $\text{mg C m}^{-2} \text{d}^{-1}$ ) was assessed by the gut  
260 fluorescence method (Meddeb et al., 2018; Tseng et al., 2008) The experimental procedure and the  
261 calculations are detailed in Chkili et al. (2023). Sinking fluxes were estimated by collecting organic  
262 particles (NAN, MIC, DET and MET fecal pellets) that settle down along the water column in  
263 sediment traps moored at two meters from the bottom of each station. The deployment of sediment  
264 traps, the analyses of their contents and the calculation of the vertical fluxes of each type of particle  
265 are described in Chkili et al. (2023).

#### 266 **2.4. Model development**

267 Field data provide a limited number of known fluxes. To have a complete model of planktonic  
268 food webs, the LIM-MCMC method (Meersche et al., 2009) was used to construct carbon fluxes  
269 between planktonic compartments at the four stations. This approach is based on four steps: (i)  
270 constructing an *a priori* model, (ii) setting the equalities, (iii) setting the inequalities, and (iv)  
271 calculating possible solutions for each flux.

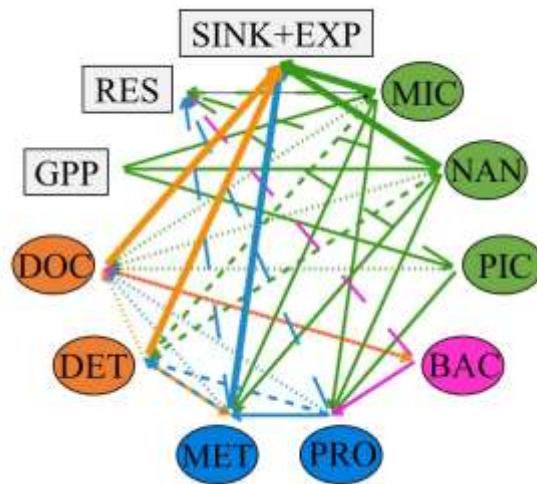
272           **2.4.1. *A priori* model**

273           The *a priori* model included planktonic compartments and all possible known and  
274 unknown carbon fluxes between them. In each station, the model included eight compartments:  
275 BAC, PIC, NAN, MIC, PRO (mainly protozoans < 200 µm: heterotrophic nanoflagellates,  
276 dinoflagellates and ciliates), MET (mainly metazoans > 200 µm), DOC and DET. The model  
277 encompassed thirty-five fluxes between the compartments and their outside (Fig. 2). Gross  
278 primary production (GPP) of the three phytoplankton size fractions (PIC, NAN and MIC) was  
279 the only source of carbon input to the network. Some of this carbon was lost by respiration  
280 (RES) by all living compartments, sinking (SINK) of most compartments (except BAC, PIC  
281 and PRO), and DOC export (EXP). It was assumed that the very small size of PIC and BAC  
282 did not allow them to generate a sinking flux. Dissolution of detritus, exudation by  
283 phytoplankton and excretion by zooplankton (PRO and MET) contribute to DOC formation.  
284 BAC were the only users of DOC since other potential DOC consumers such as  
285 choanoflagellates were absent in our samples (Chkili et al., 2023). All living compartments but  
286 PIC and BAC contributed to generate DET through mortality, production of faecal pellets by  
287 MET and sloppy feeding by zooplankton. Concerning trophic interactions, BAC and all  
288 phytoplankton size fractions were consumed by PRO, while MET only consumed NAN and  
289 MIC because smaller cells (BAC and PIC) are inefficiently captured by MET (Fortier et al.,  
290 1994). PRO and DET also contributed to a food source for MET.

291

292

293



295

296 **Fig. 2.** *A priori* food web model for the four stations. Colored circles represent internal  
297 compartments. Green, primary producers (PIC = picophytoplankton < 2  $\mu\text{m}$ , NAN =  
298 nanophytoplankton 2-10  $\mu\text{m}$ , MIC = microphytoplankton 20-200  $\mu\text{m}$ ); pink,  
299 bacterioplankton (BAC); blue, consumers (PRO = protozooplankton, MET =  
300 metazooplankton); orange, non-living carbon (DET = detritus, DOC = dissolved organic  
301 carbon). Gray boxes correspond to external connections: carbon inputs (gross primary  
302 production, GPP) and outputs (respiration, RES; particle vertical sinking, SINK;  
303 DOC export, EXP). The arrow color of each flow refers to its source.

304

305

#### 306 2.4.2. Equalities and inequalities

307 The setting up of the equalities is an essential phase for establishing the mass balances of  
308 the network. If the mass of the compartment is constant during the period under consideration,  
309 the sum of the ingoing fluxes should be equal to the sum of the outgoing fluxes. However, the  
310 daily variations in biomass with respect to the daily flux values were neglected. A mass balance  
311 equation was written for each compartment (Table A.1).

312 The subsequent step was to impose ecological limits (maximum and/or minimum) for  
313 each unknown flux to reduce the range of possible solutions. The inequalities represented two  
314 types of ranges. The first range considered the average values of the fluxes measured in the  
315 field (i.e., production rates of BAC, PIC, NAN and MIC; grazing rates by PRO and MET, and



316 vertical sinking of particles). These average values did not allow the model to estimate flows  
317 with certainty. Therefore, we proposed to define the minimum and maximum values for each  
318 flux by calculating a confidence interval around the field data, i.e., by using the minimum and  
319 maximum of the mean value of each flux. In doing so, we followed the method recently  
320 developed in the LIM-MCMC applications, that considers all local data as ranges, with two  
321 inequalities for minimum and maximum values instead of equations, in order to consider the  
322 confidence of the estimation (e.g. [Nogues et al., 2021](#)).

323 Thirteen inequalities derived from field measurements were considered for every station  
324 ([Table A.2](#)). A second group of constraints was adopted from the literature to constrain the  
325 unknown fluxes ([Vézina and Piatt, 1988](#); [Steinberg et al., 2000](#); [Vézina and Pahlow, 2003](#)).  
326 These inequalities included the lower and/or upper limits of several processes such as  
327 respiration of all living compartments; DOC production by phytoplankton, PRO, MET and  
328 BAC; production and dissolution of DET; growth efficiency of BAC, PRO and MET, and  
329 assimilation efficiency of PRO and MET. For preferential ingestion by MET, we used diet  
330 constraints, which are based on the assumption that MET feeding depends on the availability  
331 of their prey, i.e., the abundance of a prey relative to other prey ([Haraldsson et al., 2018](#)). The  
332 availability ( $A$ , as a fraction) of prey compartment  $i$  to consumer compartment  $j$  was calculated  
333 based on the specific diet data about each species  $k$  in the consumer compartment:

$$334 \quad A_{ij} = \sum_{k=0}^n \left( \frac{\text{prey}_{ijk} \times SC}{\sum \text{prey}_{ijk}} \times \frac{\text{consum}_{jk}}{\sum \text{consum}_{jk}} \right)$$

335  
336 where prey and consum are the biomasses of the prey and consumer, respectively, SC is the  
337 selection coefficient (= 1 when there was no selection, = 1.4 when there was assumed positive  
338 selection, and = 0.6 when there was negative selection) ([Table A.3](#)). Twenty-six inequalities  
339 from this second group were applied in the model to the four stations ([Table A.3](#)).



### 340 2.4.3. Solutions

341 The calculation of the unknown fluxes was the last step of the inverse analysis. The LIM-  
342 MCMC method based on the mirror technique defined by Meersche et al. (2009) estimates each  
343 unknown flux. Two parameters must be specified to use this technique: the number of iterations  
344 to be used to maximize the exploration (or coverage) of the polytope of solutions, and the jump  
345 value – the average distance between two successive solutions in a randomly chosen direction.  
346 For the present study, a jump value of  $10 \text{ mg C m}^{-2} \text{ d}^{-1}$  and 300,000 iterations were adopted to  
347 run the models and optimize the coverage of all possible solutions.

### 348 2.5. Food web typology ratios

349 To describe the different interactions between compartments and identify the type of  
350 trophic pathway, Sakka Hlaili et al. (2014) provided seven operational criteria based on carbon  
351 flux ratios that can be easily estimated in the field. In our study, four food web typology ratios  
352 were calculated from the flux data yielded by the models (Table 1). Ratio R4 (total net  
353 phytoplankton production divided by the net production of potential food for PRO) determined  
354 the relative importance of phytoplankton production, while ratio R6 (net production of DOC  
355 and DET divided by the net production of potential food for PRO) expressed the significance  
356 of production by non-living compartments. Ratio R7 (picophytoplankton net production  
357 divided by total phytoplankton net production) discriminated between herbivorous ( $R7 \leq 0.1$ ),  
358 multivorous ( $0.1 < R7 < 0.6$ ) and microbial food webs ( $R7: \geq 0.6$ ). Ratio R8 (consumption rate  
359 of total phytoplankton by PRO divided by the consumption rate of total phytoplankton by PRO  
360 and MET) identified the main phytoplankton grazers (i.e., PRO when  $R8 > 0.5$  or MET when  
361  $R8 < 0.5$ ).

362

363

364 **Table 1.** Carbon flow ratios for the determination of planktonic food web types (Sakka Hlaili  
 365 et al., 2014). PIC, Picophytoplankton; PRO, Protozooplankton; MET, Metazooplankton;  
 366 DOC, Dissolved Organic Carbon; DET, Detritus.

Ratio	Formula	Description	Trophic interpretation
Ratio 4 (R4)	$P_{netpht}/D2^{**}$	Total net phytoplankton production divided by net production of potential (PRO) feed	Phytoplankton contribution to production of potential protozooplankton feed
Ratio 6 (R6)	$(P_{netDET} + P_{netDOC})/D2$	Net production of DOC and DET divided by net production of potential PRO food	Contribution of non-living organic matter to production of potential PRO feed
Ratio 7 (R7)	$P_{netPIC}/P_{netpht}$	Net PIC production divided by total net phytoplankton production	PIC contribution to total net phy production
Ratio 8 (R8)	$pht-PRO/(pht-PRO + pht-MET)$	Consumption rate of total phytoplankton by PRO divided by consumption rate of total phytoplankton by PRO and MET	Importance of PRO in the consumption of total phytoplankton

367 \*Pnet = Net production, pht = Total phytoplankton  
 368 \*\*D2= Pnetpht + PnetBAC + PnetDET + PnetDOC  
 369

## 370 2.6. Ecological network analysis (ENA)

371 An ecological network analysis (ENA) was applied to describe the functioning of the  
 372 ecosystem from the flux values obtained by the LIM-MCMC approach. ENA examines the food  
 373 web structure within the ecosystem and its emerging properties (Ulanowicz, 1986; Fath and  
 374 Patten, 1999; Tecchio et al., 2015; Meddeb et al., 2019). A number of calculated indices were  
 375 considered to compare and characterize the stations:

376 - **Total system throughput (TST):** The total system throughput is the sum of all fluxes through  
 377 all compartments (Kay et al., 1989). The TST is interpreted as an indicator of the system activity  
 378 (Rutledge et al., 1976; Latham, 2006) and is calculated as:

$$379 \quad TST = \sum_{i=1, j=1}^n T_{ij}$$

380 Where  $T_{ij}$  is the flux from compartment  $i$  to compartment  $j$ . The size of the system is associated  
 381 with its level of activity, which is determined by the number of compartments and the  
 382 magnitude of the fluxes (Bodini et al., 2012; Ulanowicz, 1986).

383 - **Average mutual information (AMI):** This index measures the efficiency with which materials  
384 are transported through the network. It describes the organization of exchanges between  
385 compartments (Latham and Scully, 2002; Ulanowicz, 2004) and is expressed as follows:

$$386 \quad AMI = \sum_{i=1, j=1}^n T_{ij} Q_i \log \left( \frac{T_{ij}}{\sum_{k=1} T_{kj} Q_k} \right)$$

387 with  $T_{ij}$  is the flux from compartment  $i$  to compartment  $j$ ;  $Q_i$  is the probability of a unit of energy  
388 passing through  $i$ ; and  $T_{kj}$  and  $Q_k$  represent the total flux of  $j$  and the probability of a unit of  
389 energy passing through other compartments. Low values of AMI indicate that the system is  
390 evolving towards a web-like food web, while high values show an increase in  
391 specialization/constraints (Ulanowicz, 1997, 2004).

392 - **Ascendency/Development Capacity (A/C) ratio:** The A/C ratio shows the degree of  
393 organization of the food web (Ulanowicz et al., 2009). Ascendency (A) represents the organized  
394 part of the ecosystem and is more informative when expressed in relation to the development  
395 capacity (relative Ascendency, A/C). The development capacity (C) represents the maximum  
396 possible value of Ascendency that an ecosystem can reach.

397 It is calculated as follows:

$$398 \quad A/C = \frac{AMI * T..}{-\sum_{ij} t_{ij} \log \left( \frac{t_{ij}}{T} \right)}$$

399 - **Finn cycling index (FCI):** The FCI (Finn, 1976) represents the fraction of the total flux  
400 through the system that is cyclic, i.e., the proportion of the flux that revisits the same node  
401 several times before exiting the system. The recycled flux from node  $i$  ( $TST_{ci}$ ) can be calculated  
402 from the following equation:

$$403 \quad TST_{ci} = \left( \frac{n_{ii} - 1}{n_{ii}} \right) T_i$$

404 Thus, the FCI can be calculated by dividing the total cycling flux ( $TST_{ci}$ ) by the total system  
405 throughput (TST):

$$406 \quad FCI = \sum TST_{ci} / TST_{flux}$$

407 - **Average path length (APL):** The APL is the mean number of compartments crossed by a  
408 carbon unit from its entry to its exit from the system. It is an indicator of the amount of system  
409 activity ( $TST_{flow}$ ) generated by each unit input into the system (Finn, 1976). It is calculated as  
410 follows:

$$411 \quad APL = \frac{TST_{flux}}{\sum_{i=1}^n z_i}$$

412 APL is an indicator of the amount of system activity ( $TST_{flux}$ ) generated by each unit of input  
413 to the system. Thus, Jørgensen et al. (2000) interpreted this index as an indicator of the growth  
414 and development of the system, which they renamed network aggradation since it forms an  
415 indicator of the organization of the system and its capacity to do more work with given  
416 resources (the input limit).

417 - **Detritivory/herbivory (D/H) ratio:** The D/H ratio measures the importance of grazing of  
418 phytoplankton relative to detrital carbon consumption. It is a simple ratio where detritivory  
419 represents the DET-MET and DOC-BAC fluxes and herbivory represents phytoplankton  
420 consumption fluxes by PRO and MET (Kay et al., 1989; Ulanowicz, 1992; Baird et al., 2009).

## 421 2.7. Statistical analyses

### 422 2.7.1. Multiple factor analysis (MFA)

423 A multiple factor analysis (MFA) was performed to identify the interrelationships  
424 between different ecological indicators (food web typology ratios and ENA indices) as well as  
425 environmental variables (inorganic and organic nutrients) and some of the calculated fluxes  
426 (GPP of PIC, NAN and MIC, bacterial production and sinking of NAN, MIC and MET). Each  
427 station was considered as a group, which by definition included variables measured at the same

428 date. The objective was to find a common or representative structure for all groups. Unlike  
429 individual principal component analysis, MFA can integrate groups of variables (at different  
430 sampling dates) in a single analysis, and analyzes the relationship within each group and over  
431 time (Escofier and Pagès, 1990).

432 The calculated indices as well as the environmental and biological data determined in the  
433 water column were organized in a matrix where the rows (individuals) represented the 50  
434 randomly chosen values of LIM solutions and the columns (identified variables) were the  
435 parameters determined in each station. There were 200 individuals (or rows) in total, and 21  
436 variables were used for each sample. The analysis consisted of a principal component analysis  
437 for each table, weighted by dividing each variable by its PCA eigenvalue for the final analysis.  
438 Four tables were considered: ENA indices, typology ratios, primary and bacterial production,  
439 and export.

440 All modeling and statistical analyses were performed in R software with LIM libraries  
441 for linear inverse modeling, NetIndices for ENA calculation as well as FactomineR, Ade4 and  
442 vegan for digital analyses of the results.

### 443 2.7.2. Cliff's $\delta$ test for comparing network indices between stations

444 The Cliff's  $\delta$  test was used to statistically test ENA index differences between models (Tecchio  
445 et al., 2016). This method is necessary for large sample sizes (in our case 300,000 values for  
446 each stream). Four pairwise comparisons were performed for each ENA index. Then, the  
447 following values were used to define small, medium, and large effects (small,  $|\delta| \geq 0.11$ ;  
448 medium,  $|\delta| \geq 0.28$ ; large,  $|\delta| \geq 0.43$ ; Vargha and Delaney, 2000; Romano et al., 2006).

## 449 3. Results

### 450 3.1. Input, output and throughput flows

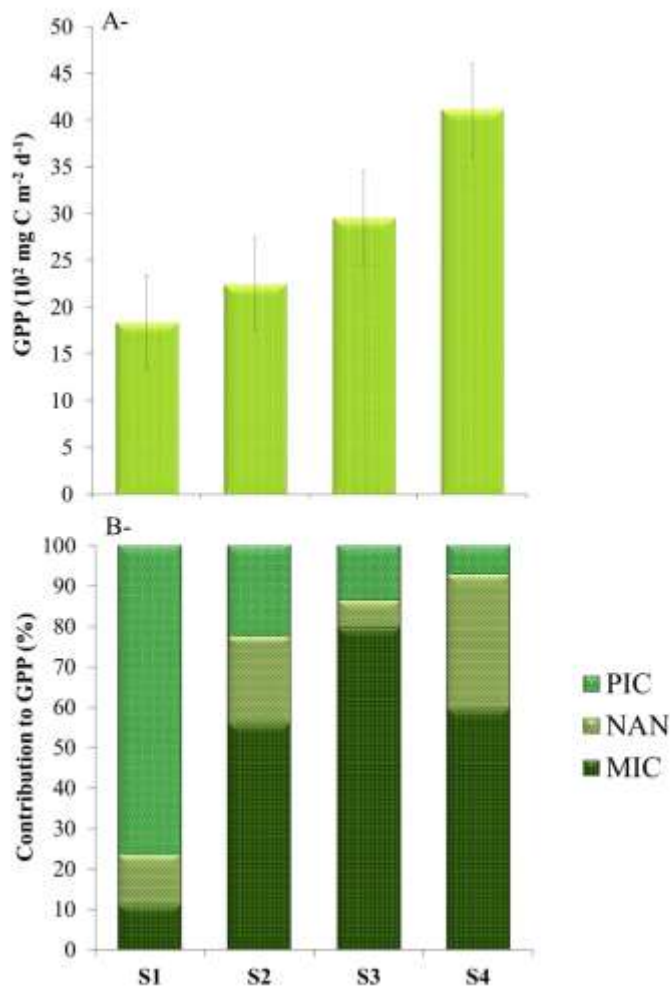
451 We calculated 34 carbon flows in each station using LIM-MCMC analysis (Table 2).  
452 Phytoplankton gross primary production (GPP) was the only carbon input in the food web.

453 Total GPP followed an ascending gradient from S1 (1,838.5 mg C m<sup>-2</sup> d<sup>-1</sup>), then S2, S3 (2,240.2  
 454 - 2,954 mg C m<sup>-2</sup> d<sup>-1</sup>) up to S4 (4,110.1 mg C m<sup>-2</sup> d<sup>-1</sup>) (Fig. 3 A). The contribution of each  
 455 phytoplankton size fraction to total GPP varied among stations (Fig. 3 B). PIC was the main  
 456 producer in S1 (76%), versus MIC in the other stations (56-80%). The contribution of NAN  
 457 was low (7-21%), but reached 33% in S4.

458 **Table 2.** Mean values of the fluxes estimated by the Monte Carlo Markov chain inverse linear  
 459 modeling (LIM-MCMC) approach for each station in the Gulf of Gabès.

Flow description	Symbol	estimated value (mg C m <sup>-2</sup> d <sup>-1</sup> )			
		S1	S2	S3	S4
Microphytoplankton gross primary production	GPP-MIC	206.40	1258.00	2359.00	2451.00
Nanophytoplankton gross primary production	GPP-NAN	228.10	481.00	195.70	1365.00
Picophytoplankton gross primary production	GPP-PIC	1404.00	501.20	339.30	294.10
Microphytoplankton respiration	MIC-RES	11.24	78.49	151.70	167.70
Microphytoplankton dissolved organic carbon exudation	MIC-DOC	20.35	144.77	333.20	268.00
Microphytoplankton net production	MIC-DET	0.91	175.88	1259.60	72.48
Microphytoplankton grazing by protozooplankton	MIC-PRO	64.78	441.70	310.90	994.00
Microphytoplankton grazing by metazooplankton	MIC-MET	58.07	281.80	209.80	650.50
Microphytoplankton sinking	MIC-LOS	51.03	135.00	93.60	298.50
Nanophytoplankton respiration	NAN-RES	19.67	39.65	21.41	131.43
Nanophytoplankton dissolved organic carbon exudation	NAN-DOC	29.01	69.71	30.58	182.43
Nanophytoplankton detritus production	NAN-DET	72.82	247.80	14.12	632.50
Nanophytoplankton grazing by protozooplankton	NAN-PRO	88.33	100.93	116.70	315.20
Nanophytoplankton grazing by metazooplankton	NAN-MET	16.40	22.54	12.72	102.71
Nanophytoplankton sinking	NAN-LOS	1.92	0.37	0.14	0.49
Picophytoplankton respiration	PIC-RES	298.23	76.28	96.51	81.57
Picophytoplankton dissolved organic carbon exudation	PIC-DOC	332.50	120.73	88.99	65.67
Picophytoplankton grazing by protozooplankton	PIC-PRO	773.10	304.10	213.80	146.90
Protozooplankton respiration	PRO-RES	464.70	374.10	352.60	547.60
Protozooplankton dissolved organic carbon excretion	PRO-DOC	146.80	248.00	248.60	277.90
Protozooplankton detritus production	PRO-DET	323.60	244.00	197.40	307.70
Protozooplankton consumption by MET	PRO-MET	317.30	484.70	406.90	684.70
Metazooplankton respiration	MET-RES	147.34	353.00	203.50	575.90
Metazooplankton dissolved organic carbon excretion	MET-DOC	63.31	234.50	125.25	270.20
Metazooplankton detritus production	MET-DET	93.79	228.80	105.15	324.00
Metazooplankton sinking	MET-LOS	125.20	313.90	201.90	541.70
Bacterial respiration	BAC-RES	219.30	308.50	338.00	302.70
Bacterial dissolved organic carbon production	BAC-DOC	112.94	250.65	263.24	100.02
Bacterial grazing by protozooplankton	BAC-PRO	326.10	504.00	564.00	361.90
Dissolved organic carbon uptake by bacteria	DOC-BAC	658.30	1063.20	1165.00	764.60
Dissolved organic carbon output	DOC-LOS	54.55	29.10	38.05	460.30
Detritus dissolution	DET-DOC	8.03	26.91	113.50	60.77
Detritus consumption by metazooplankton	DET-MET	37.88	338.10	6.35	273.90
Detritus sinking	DET-LOS	445.30	531.50	1456.00	1002.00

460



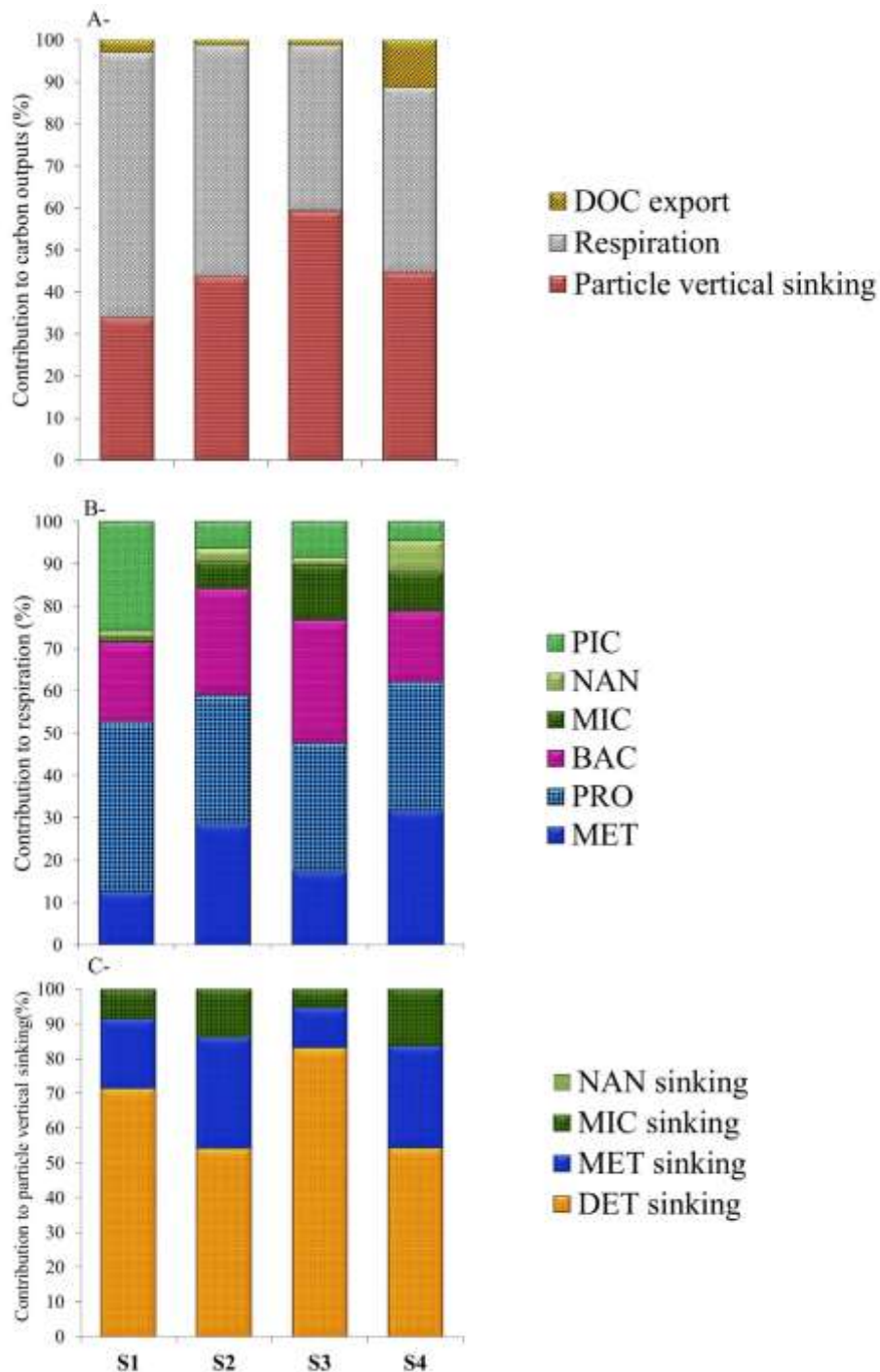
461

462 **Fig. 3.** Total gross primary production (GPP) (A), and contribution of each phytoplankton size  
463 fraction to GPP (B). PIC, picophytoplankton; NAN, nanophytoplankton; MIC,  
464 microphytoplankton.

465 The output flows were represented by respiration of all living organisms, DOC export,  
466 and particle vertical sinking of MIC, NAN, MET and DET. These outputs differed among  
467 stations (Table 2, Fig. 4 A). Respiration represented the main carbon output in S1 (63%) and  
468 S2 (55%) and to lesser extent in S3 and S4 (39-44%) (Fig. 4 A). Carbon loss through respiration  
469 was about 2-32% of GPP in S2, S3 and S4, and 1-40% in S1. PRO, MET and BAC altogether  
470 contributed 77-84% of respiration in S2, S3 and S4, while the total contribution of  
471 phytoplankton was  $\leq 23\%$ . In S1, the contribution of phytoplankton to this output increased  
472 ( $\sim 30\%$ ) due to the enhancement of PIC respiration (Fig. 4 B). DOC export was low, except in  
473 S4 where it formed 11% of the carbon output. Particle sinking provided 34-45% of total carbon  
474 loss in S1, S2 and S4, and 59% in S3 (Fig. 4 A). Particle sinking formed the second main source



475 of carbon output (43-59%). MET and MIC represented most of the living sinking particles: they  
476 represented 12-32% and 5-16% of carbon loss, respectively (Fig. 4 C).

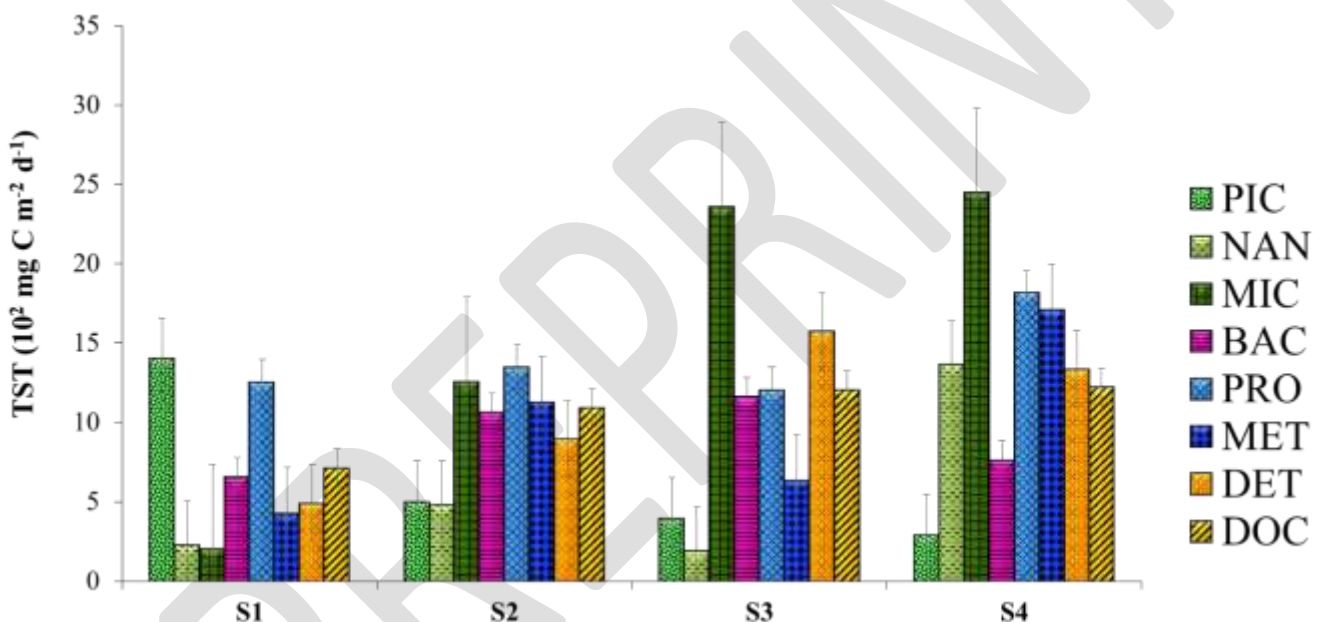


477

478 **Fig. 4.** Composition of total carbon outputs (A), contributions of living compartments to  
479 respiration (B) and contributions of living and non-living compartments to carbon  
480 sinking (C) in four stations in the Gulf of Gabès. PIC, picophytoplankton; NAN,  
481 nanophytoplankton; MIC, microphytoplankton; BAC, bacterioplankton; PRO,  
482 protozooplankton; MET, metazooplankton; DET, detritus; DOC, dissolved organic  
483 carbon.

484

485 Throughput was defined as the sum of carbon flows coming into or leaving a  
486 compartment. The throughput of each compartment varied among stations (Fig. 5). In S1, PIC  
487 and PRO showed the highest value of carbon throughput ( $1,401$  and  $1,256$   $\text{mg C m}^{-2} \text{d}^{-1}$ ,  
488 respectively), while both living compartments (MIC, BAC, PRO and MET) and non-living  
489 compartments (DET and DOC) showed similar carbon throughputs in S2 ( $896$ - $1,258$   $\text{mg C m}^{-2}$   
490  $\text{d}^{-1}$ ). However, MIC had the highest throughput ( $2,451$   $\text{mg C m}^{-2} \text{d}^{-1}$ ) in S3 and S4, largely  
491 above its throughputs in S1 and S2. BAC, PRO, DET and DOC had relatively high throughputs  
492 in S3 ( $1,165$ - $1,576$   $\text{mg C m}^{-2} \text{d}^{-1}$ ), while MET and PRO had higher values ( $1,712$ - $1,818$   $\text{mg C}$   
493  $\text{m}^{-2} \text{d}^{-1}$ ) than DET and DOC ( $1,337$ - $1,225$   $\text{mg C m}^{-2} \text{d}^{-1}$ ) in S4.



494 **Fig. 5.** Throughput of each compartment for the four models of four stations in the Gulf of  
495 Gabès. TST, total system throughput; PIC, picophytoplankton; NAN, nanophytoplankton;  
496 MIC, microphytoplankton; BAC, bacteria; PRO, protozooplankton; MET, metazooplankton;  
497 DET, detritus; DOC, dissolved organic carbon.  
498  
499

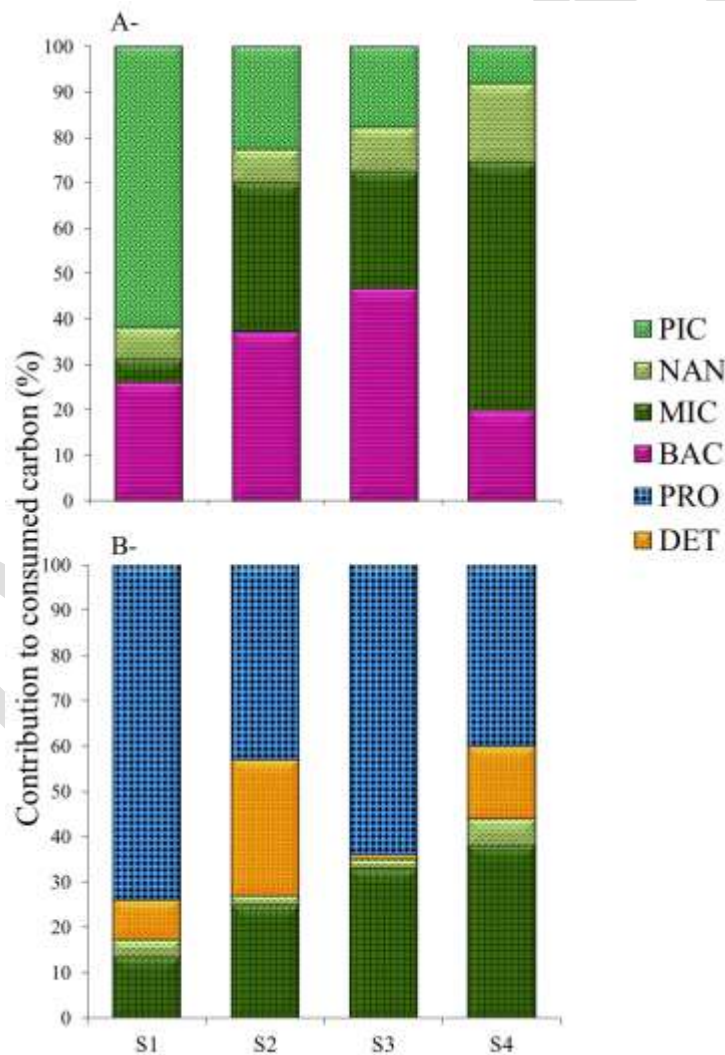
500 Error bars, 95% confidence intervals calculated from the probability of distribution of each  
501 flow and for 300,000 solutions *per* flow.

### 502 3.2. Protozooplankton and metazooplankton diets

503 The diets of PRO and MET were expressed as the contribution of each food source to the  
504 carbon consumed by grazers. The diets of both zooplankton compartments varied among  
505 stations (Fig. 6). PRO mainly fed on PIC (62%) followed by BAC (26%) in S1. In S2 and S3,

506 the diet of PRO was roughly divided between BAC (37-47%) and phytoplankton (mainly MIC:  
507 33-26% and PIC: 23-18%). Conversely, phytoplankton were the main food source of PRO in  
508 S4; MIC alone formed 54% of its diet (Fig. 6 A).

509 In S1, MET was mainly carnivorous, since PRO formed 74% of its diet, while  
510 phytoplankton only provided 17%. In S2, PRO and DET were the main food source of MET,  
511 forming 43% and 30% of its consumed carbon, respectively. In S3, the diet of MET mainly  
512 relied on PRO (64%), and MIC contributed 33%. In S4, the contribution of phytoplankton  
513 (mainly MIC) to MET diet increased to 44%. PRO formed 40% of MET diet, while DET only  
514 represented 16% in this station (Fig. 6 B).



515

516 **Fig. 6.** Diets of protozooplankton (A) and metazooplankton (B) in four stations in the Gulf of  
517 Gabès. PIC, picophytoplankton; NAN, nanophytoplankton; MIC, microphytoplankton;  
518 BAC, bacterioplankton; PRO, protozooplankton; DET, detritus.

519

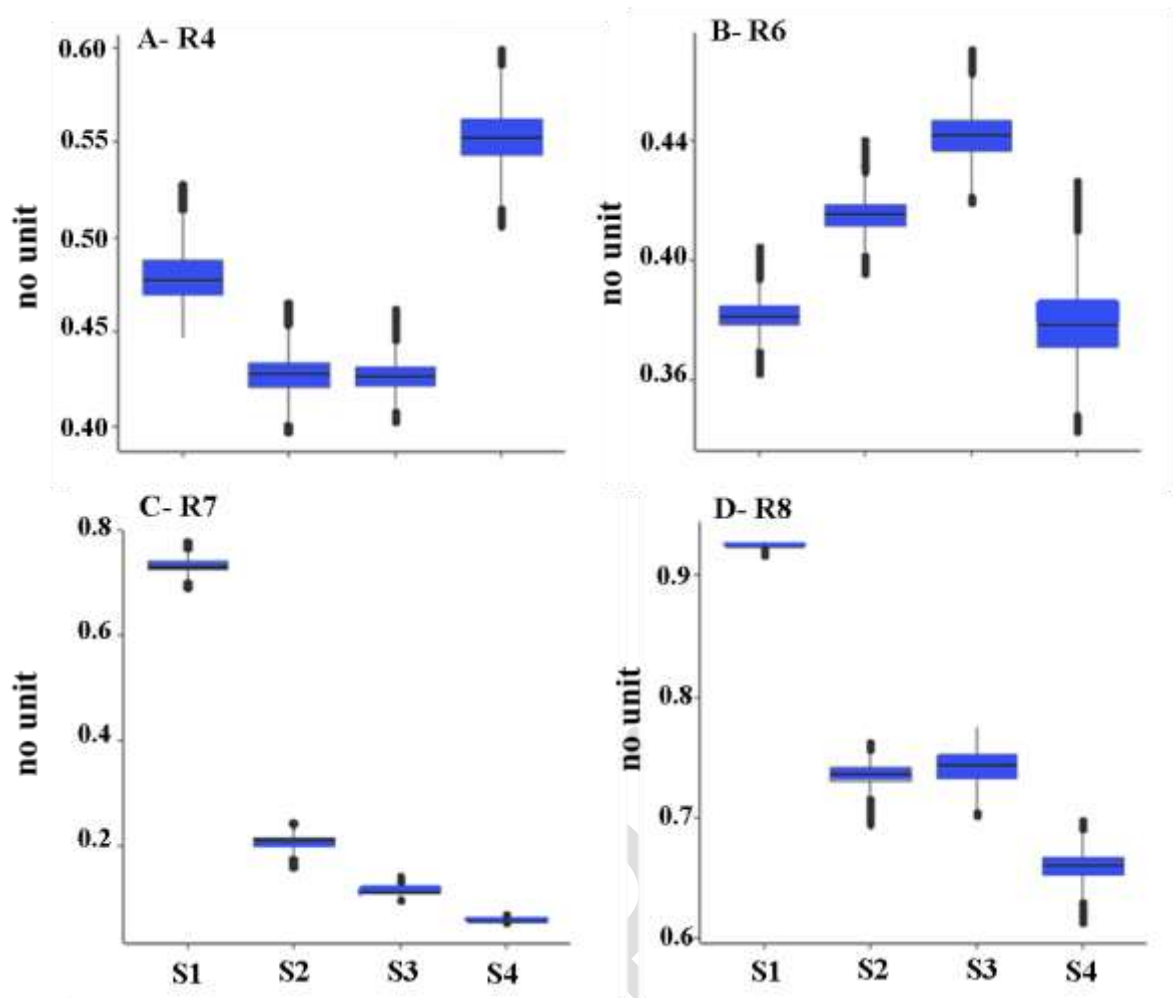
520 **3.3. Food web typology ratios**

521 The stations presented distinct carbon circulations through the food webs. The typology  
 522 ratios varied significantly among stations according to Cliff's  $\delta$  test (Table 3, Fig. 7). Ratio R4  
 523 significantly differed among stations, with higher values in S4 (0.55) and S1 (0.48) than in S2  
 524 and S3 (0.43 and 0.42, respectively) (Fig. 7 A). R6 followed an opposite trend, with lower  
 525 values in S1 and S4 (0.39 and 0.38, respectively) than in S2 and S3 (0.41 and 0.44, respectively)  
 526 (Fig. 7 B). R7 and R8 were very high in S1 (0.73 and 0.92, respectively) and decreased in S2  
 527 (0.21 and 0.74) and S3 (0.11 and 0.74) to reach their lowest values in S4 (0.06 and 0.66) (Fig.  
 528 7 C, D).

529 **Table 3.** Results of Cliffs'  $\delta$  test applied to ecological network indices and typology ratios  
 530 calculated for four stations of the Gulf of Gabès. The following values were used to define the  
 531 size of the effects:  $|\delta| \geq 0.43$ , large; \*\*\*, large.

	S1/S2	S1/S3	S1/S4	S2/S3	S2/S4	S3/S4
<b>TST</b>	-1 (***)	-1 (***)	-1 (***)	-1 (***)	-1 (***)	-1 (***)
<b>A/C</b>	1 (***)	-1 (***)	1 (***)	-1 (***)	1 (***)	1 (***)
<b>AMI</b>	1 (***)	-1 (***)	1 (***)	-1 (***)	1 (***)	1 (***)
<b>APL</b>	-0.93 (***)	0.93 (***)	1 (***)	1 (***)	1 (***)	1 (***)
<b>FCI</b>	-1 (***)	-1 (***)	0.73 (***)	0.99 (***)	1 (***)	1 (***)
<b>D/H</b>	-1 (***)	-1 (***)	1 (***)	-0.93 (***)	1 (***)	1 (***)
<b>R4</b>	1 (***)	1 (***)	-1 (***)	0.67 (***)	-1 (***)	-1 (***)
<b>R6</b>	-1 (***)	-1 (***)	0.66 (***)	-1 (***)	1 (***)	1 (***)
<b>R7</b>	1 (***)	1 (***)	1 (***)	1 (***)	1 (***)	1 (***)
<b>R8</b>	1 (***)	1 (***)	1 (***)	-0.89 (***)	1 (***)	1 (***)

532



533

534

535

536

537

538

539

540

**Fig. 7.** Spatial variation of the food web typology ratios.  
R4 =  $P_{netpht}/D2$  (A), R6 =  $(P_{netDET} + P_{netDOC})/D2$  (B), R7 =  $P_{netPIC}/P_{netpht}$  (C)  
and R8 =  $pht-PRO/(pht-PRO + pht-MET)$  (D)  
Pnet, net production; pht, total phytoplankton; D2,  $P_{netpht} + P_{netBAC} + P_{netDET} + P_{netDOC}$ ;  
pht-PRO, consumption of pht by PRO; pht-MET, consumption of pht by MET.

541

### 3.4. Ecological network analysis (ENA) indices

542

Ecological network analysis (ENA) indices define emerging properties of the food web.

543

They clearly distinguished the functioning of each station; all indices varied significantly and

544

showed large differences among stations according to Cliff's  $\delta$  test (Table 3, Fig. 8). The total

545

system flux (TST) was higher in S4 ( $10,966 \text{ mg C m}^{-2} \text{ d}^{-1}$ ) than in S2, S3 ( $7,770\text{--}8,740 \text{ mg C}$

546

$\text{m}^{-2} \text{ d}^{-1}$ ) and S1 ( $5,386 \text{ mg C m}^{-2} \text{ d}^{-1}$ ) (Fig. 8 A). Conversely, the lowest relative Ascendency

547

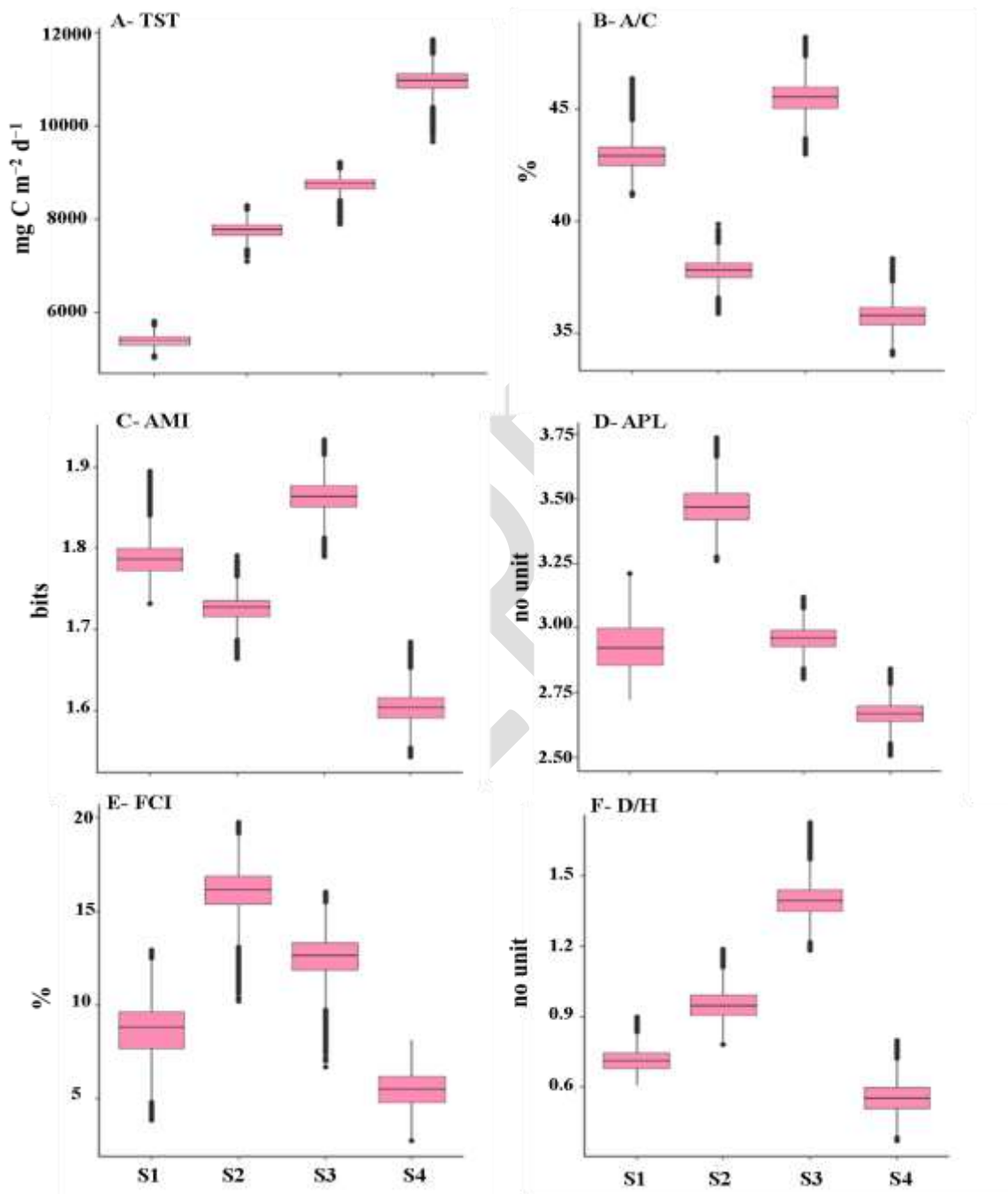
(A/C) was found for the food webs of S4 (0.32 %) in comparison with the other stations (0.38–

548

0.46 %) (Fig. 8 B). Average mutual information (AMI) followed a similar trend to that of A/C,



549 with higher values in S1, S2 and S3 (1.72-1.86 bits) than in S4 (1.60 bits) (Fig. 8 C). The  
550 average path length (APL) and Finn cycling index (FCI) showed similar spatial variations, with  
551 the highest values in S2 (3.46 and 0.16%, respectively) and the lowest ones in S4 (2.67 and  
552 0.05%, respectively) (Fig. 8 D, E). Finally, the D/H ratios in S2 and S3 (1.22-1.36) significantly  
553 exceeded those in S1 (0.70) and S4 (0.47) (Fig. 8 F).



554

555 **Fig. 8.** Spatial variation of ENA indices calculated for the planktonic food webs in four stations  
556 of the Gulf of Gabès. Total system throughput (TST; mg C m<sup>-2</sup> d<sup>-1</sup>) (A), relative  
557 Ascendency (A/C; %) (B), average mutual information (AMI; bits) (C), average path  
558 length (APL) (D), cycling index (FCI; %) (E), and detritivory to herbivory (D/H) (F).

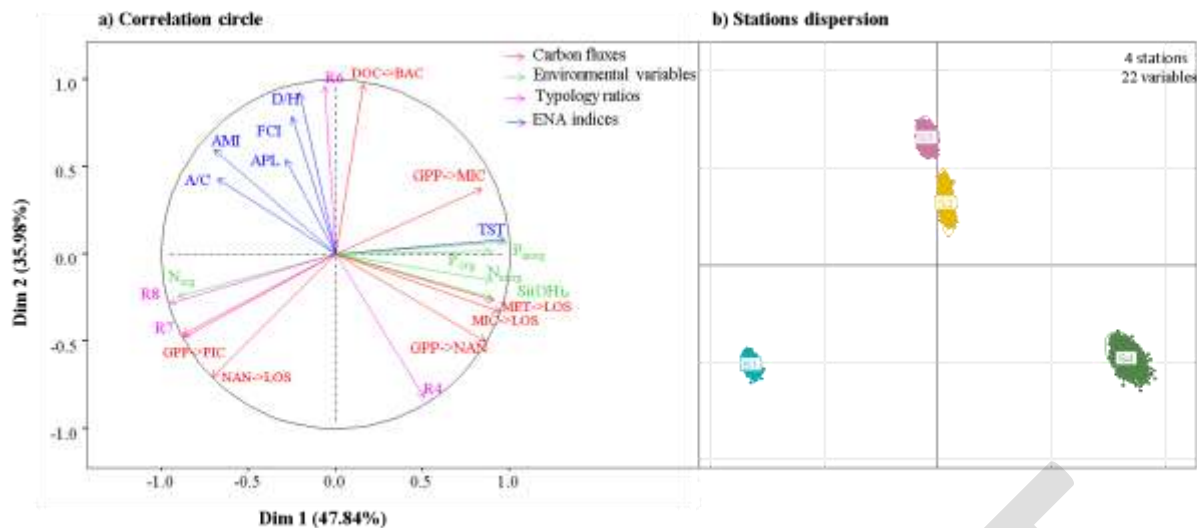
559 **3.5. Relationships between ENA indices, typology ratios, input and output flows and**  
560 **environmental variables**  
561

562 Multiple factor analysis (MFA) was applied to the four stations on ENA indices, carbon  
563 flux ratios, inorganic and organic nutrients, size-fractionated GPP, bacterial production and  
564 particle sinking (Fig. 9). The first two axes of the MFA explained 47.84% and 35.98% of the  
565 total variance, respectively.

566 On the first axis of the MFA, the TST index (5%), GPP of NAN (6%) and MIC (6%),  
567 sinking of MIC (7%) and MET (7%) and nutrients ( $N_{inorg}$  3%,  $P_{org}$  and  $P_{inorg}$  3-4%,  $Si_{inorg}$  4%)  
568 were projected onto its positive pole. Its negative pole was determined by the A/C index (2%),  
569 ratios R7 (6%) and R8 (8%), GPP of PIC (6%), sinking of NAN (6%) and  $N_{org}$  (4%) The  
570 positive pole of the second axis was related to several ENA indices (D/H 6%, FCI 4%, APL  
571 2%, AMI 2%, and A/C 2%), R6 (10%) and bacterial production (23%), while its negative pole  
572 was related to R4 (7%) (Fig. 9 A).

573 Stations S1 and S4 were discriminated on the first axis. S1 projected on the negative  
574 pole of the axis was characterized by high values of PIC GPP and ratios R7 and R8, but hosted  
575 low concentrations of inorganic N, P and Si and low TST, indicating a poorly rich nutrient  
576 system dominated by small producers. S4 was at the opposite of S1. It was characterized by  
577 high values of GPP for MIC and NAN, inorganic nutrient concentrations, TST and sinking of  
578 MIC and MET. Stations S2 and S3 occupied the center of axis 1, indicating that the factors  
579 represented on axis 1 were not discriminating for these stations. However, S2 and S3 were  
580 projected on the positive pole of axis 2 and were characterized by high values of BAC  
581 production, D/H and FCI indices and R6, but a low R4 (Fig. 9 B).





582

583 **Fig. 9.** Multiple factor analysis (MFA) ordination diagram showing the relationships between  
584 ecological indicators (food web typology ratios and ENA indices), environmental variables  
585 (inorganic and organic nutrients: N<sub>inorg</sub>, P<sub>inorg</sub>, Si<sub>inorg</sub>, N<sub>org</sub>, P<sub>org</sub>) and carbon flows [GPP of  
586 PIC (GPP->PIC), NAN (GPP->NAN) and MIC (GPP->MIC), bacterial production (DOC->  
587 BAC) and sinking of NAN (NAN->LOS), MIC (MIC->LOS) and MET (MET->LOS)].

## 588 4. Discussion

### 589 4.1. Spatial change in planktonic food web characteristics

590 The complex hydrodynamic circulation in the Gulf of Gabès coupled with anthropogenic  
591 nutrient inputs created a north-south and coast-offshore ascending gradient of nutrients that  
592 induced a spatial change in the size community structure of phytoplankton (Chkili et al., 2023).  
593 As expected, the present study also showed a clear spatial variation of primary production, in  
594 quantity (Fig. 3 A) and composition (Fig. 3 B). Nutrients are always considered as the main  
595 factor controlling the size structure of primary producers, which in turn influence the food web  
596 organization (Legendre and Rassoulzadegan, 1995; Sakka Hlaili et al., 2008; Filiz et al., 2020;  
597 Hardikar et al., 2021). It is well admitted that identifying the dominant phytoplankton size  
598 fractions could play a crucial role in predicting food web types (Richardson and Jackson, 2007).  
599 For example, Bellinger et al. (2006) and Hardikar et al. (2021) highlighted that the size fraction  
600 of producers, i.e., small *versus* large phytoplankton, could be used as a robust indicator of the  
601 trophic level of the system and the carbon transfer pathway. In our study, nutrients appeared as  
602 significant environmental discriminant factors of the stations, in which small and large

603 phytoplankton played different roles in biogenic carbon production (MFA, Fig. 9). In addition,  
604 the increase in large phytoplankton relative to small cells can be an indicator of eutrophication  
605 (Bell and Elmetri, 1995; Garmendia et al., 2011; Machado et al., 2023). Nano and micro-  
606 phytoplankton were indeed dominant in S4 – the most nutrient-rich station –, which could  
607 confirm the eutrophication status of this station.

608 Phytoplankton size structure and production can change rapidly in response to  
609 environmental and anthropogenic disturbances such as vertical mixing patterns, light and  
610 temperature fluctuations, salinity or nutrient availability, together with industrial, urban and  
611 agricultural discharges. These changes are obviously followed by modifications in the  
612 composition and structure of zooplankton communities and their grazing activity (Legendre  
613 and Rassoulzadegan, 1995b; Kiørboe et al., 1996; Horňák et al., 2005; Bel Hassen et al., 2008;  
614 Drira et al., 2018), which could have significant effects on the structure of the marine food web  
615 (Froneman, 2004; Legendre and Rassoulzadegan, 1995; Vargas and González, 2004;  
616 Decembrini et al., 2009; Meddeb et al., 2019). The proto- and meta-zooplankton communities  
617 indeed varied from S1 to S4, and so did their microbivory and herbivory activities (Fig.6; Table  
618 2).

619 Then, by looking at the size structure of phytoplankton, production, and the microbivory  
620 and herbivory of zooplankton, we can suggest that various food webs with different efficiencies  
621 in carbon export exist in the four stations. Going further with digital tools, we can identify the  
622 types of food web and characterize the emerging properties of each type.

#### 623 **4.2. Application of typology ratios and ENA indices to a description of the structure** 624 **and function of planktonic trophic pathways**

625  
626 Typology ratios based on the size structure of the planktonic community as well as the  
627 interactions between the different compartments are useful to distinguish planktonic trophic  
628 pathway (PTP) types in marine systems (Sakka Hlaili et al., 2014).

629 In our study, all typology ratios showed significant spatial change (Table 3, Fig. 7),  
630 suggesting variation in the structure of PTP among stations. The spatial change in R7 (Fig. 7  
631 C) evidenced a modification of the food web type among stations. In accordance with the range  
632 of R7 values given by Sakka Hlaili et al. (2014) and describing the importance of PIC in total  
633 carbon production, the microbial food web dominated in S1 ( $R7 = 0.7 > 0.6$ ), while multivorous  
634 pathways prevailed in S2 and S3 ( $0.1 < R7 = 0.2-0.12 < 0.6$ ), but the food web in S4 acted as a  
635 herbivorous type ( $R7 = 0.06 < 0.1$ ). This is in agreement with our observations of a high  
636 microbivory in S1, a shared role between microbivory and herbivory in carbon transfer in S2  
637 and S3, and a strong herbivory in S4. In addition, PIC formed the most active compartment in  
638 S1, followed by PRO, while MIC was the most active compartment in the other stations,  
639 followed by PRO and MET (Fig. 5). This suggests an important role of these communities as  
640 producers (PIC and MIC) and grazers (PRO and MET). Furthermore, R8, which distinguished  
641 the main grazers in carbon channeling (i.e., PRO *versus* MET) corroborated R7. The high R8  
642 in S1 ( $\sim 1$ ) indeed denoted that the main phytoplankton grazers in the microbial food web were  
643 PRO, while the lower values (0.66-0.74) found in the other stations (Fig. 7 D) indicated that  
644 PRO and MET altogether played an important role in carbon transfer when the dominant food  
645 web was herbivorous or multivorous. In addition, the relative importance of phytoplankton or  
646 non-living matter (DOC and DET) relatively to carbon production was specified by two other  
647 typology ratios – R4 and R6. Higher R4 than R6 values suggest that the system mainly relies  
648 on phytoplankton production, while the opposite means that non-living matter is important in  
649 circulating carbon production (Sakka Hlaili et al., 2014). These two ratios evolved differently  
650 among stations (Table 3, Fig. 7 A, B), showing that phytoplankton and/or non-living matter  
651 played different roles in carbon production across the three observed PTP. The higher R4  
652 compared to R6 in S1 indicated that the microbial food web was more based on phytoplankton  
653 (mainly PIC) than on non-living matter. This coincides with a higher throughput of  
654 phytoplankton ( $1,838.5 \text{ mg C m}^{-2} \text{ d}^{-1}$ ) than DOC and DET ( $1,204.05 \text{ mg C m}^{-2} \text{ d}^{-1}$ ) in this station  
655 (Fig 5). In the herbivorous pathway of S4, phytoplankton (mainly MIC) also played a more

656 important role ( $R4 > R6$ ) and had a higher throughput ( $4,110.1 \text{ mg C m}^{-2} \text{ d}^{-1}$ ) than non-living  
657 compartments did ( $2,561.7 \text{ mg C m}^{-2} \text{ d}^{-1}$ ) (Figs. 4, 6 A, B). For the multivorous food web  
658 observed in S2 and S3, these same R4 and R6 values suggested that the systems were based on  
659 phytoplankton as well as on non-living matter. In both stations, non-living carbon throughputs  
660 ( $1,988.74\text{-}2,779.63 \text{ mg C m}^{-2} \text{ d}^{-1}$ ) were close to phytoplankton throughputs ( $2,240.2\text{-}2,954$   
661  $\text{mg C m}^{-2} \text{ d}^{-1}$ ) (Fig. 5). Unfortunately, despite the importance of these ratios, their application  
662 is rather limited in the literature. Therefore, it would be interesting to use these criteria more  
663 extensively by comparing them with those of other ecosystems. Using these criteria, researchers  
664 and managers can identify the dominant trophic pathway in a planktonic assemblage and  
665 determine the fate of the carbon that passes through it: they can identify the main trophic  
666 pathway (i.e. herbivorous, multivorous or microbial food webs) using ratio R7, identify the  
667 main consumers of total phytoplankton using ratio R8, and specify whether the system is rather  
668 based on non-living material or phytoplankton using ratios R4 and R6 (Sakka Hlaili et al.,  
669 2014).

670 ENA indices were also used to characterize PTPs, as they are powerful tools for  
671 understanding carbon circulation through the whole food web (Ulanowicz, 1986; Ulanowicz et  
672 al., 2009). In fact, both ecological indicators (typology ratios and ENA indices) could be  
673 discriminant in the description of the food web structure (Fig. 9). However, coupling ENA  
674 indices and typology ratios required selecting complementary indices.

675 ENA indices are potentially powerful tools when assessing ecosystem health (Niquil et  
676 al., 2014) and are sensitive to different impacts on marine ecosystems (Baird et al., 2009;  
677 Tecchio et al., 2016; Pezy et al., 2017). However, they can only partially capture the  
678 anthropogenic or natural stress levels of different types of food webs in aquatic ecosystems  
679 (Tecchio et al., 2016). Therefore, food web types can also be used as an indicator of the stress  
680 level in the ecosystem and its carbon transfer capacity (Legendre and Rassoulzadegan, 1995;  
681 Siokou-Frangou et al., 2010). For example, when a microbial food web exists, particularly in

682 oligotrophic environments, primary production is maintained through recycled nutrients and is  
683 mostly lost through remineralization (Goldman et al., 1987; Legendre and Rassoulzadegan,  
684 1995; Meddeb et al., 2018). This may demonstrate stress of the system, which has become  
685 inefficient in carbon transfer (López-Abbate et al., 2019). In contrast, when herbivorous or  
686 multivorous food webs dominate, primary production is based on nutrient inputs and  
687 significantly transferred to large consumers or efficiently exported to deep waters (Michel et  
688 al., 2002; Turner, 2002). Herbivorous food webs are known for their strong capacity to channel  
689 carbon to higher pelagic and benthic consumers: low carbon is recycled (Legendre and  
690 Rassoulzadegan, 1995; Meddeb et al., 2019), indicating a stable ecosystem (Meddeb et al.,  
691 2019). Based on these statements, our study highlights the links between ecosystem typology  
692 and properties derived from ENA indices that characterize the system's activity, stability,  
693 maturity and organization.

694 The TST index is a measure of ecosystem activity and is considered as a basic index of  
695 food web models used to discriminate food webs (Finn, 1976; Ulanowicz, 1986; Borrett and  
696 Scharler, 2019). Several works have showed that high TST values correspond to productive  
697 ecosystems, such as coastal areas influenced by nutrient-rich upwelling or riverine inputs and  
698 productive continental shelves (Coll et al., 2007; Grami et al., 2008; Corrales et al., 2015;  
699 Meddeb et al., 2018). TST varied significantly among the three PTPs found in our study  
700 (Table 3, Fig. 8 A). This can obviously be linked to the variations in GPP and in the eutrophic  
701 degree of the stations. Like GPP, TST followed an increasing gradient from the least nutrient-  
702 rich station dominated by the microbial food web (S1) to the highly eutrophic station governed  
703 by the herbivorous pathway (S4). Our results corroborate other studies showing that the  
704 herbivorous food web is more active than the microbial and multivorous food webs (Meddeb  
705 et al., 2019; Decembrini et al., 2021).

706 Relative Ascendency (A/C) is an indicator of the degree of ecosystem organization  
707 (Ulanowicz, 1997; Patrício et al., 2004) that negatively correlates to the degree of maturity

708 (Christensen et al., 2005). The highest A/C value was recorded in S3 (Fig. 8 B), indicating that  
709 the multivorous pathway in this station was more organized than the food webs of the other  
710 stations. More particularly, A/C was lowest in contrast to TST in S4 and its herbivorous  
711 pathway, indicating a more active but less organized system. The AMI index is a measure of  
712 flow specializations within a system (Ulanowicz, 1986). It yields lower values at the early  
713 stages of ecosystem development (when the system is immature) and higher values under  
714 pristine conditions (least disturbed ecological functioning). In our study, AMI followed the  
715 same trend as A/C, i.e., highest in S3 and lowest in S4 (Fig. 8 C). This means that higher fluxes  
716 of BAC and DET, in parallel to MIC, may allow a greater fraction of the total system flux to  
717 pass through specialized pathways in the multivorous food web of S3. Other ENA indices that  
718 reflect stability, maturity and organization varied significantly according to the different PTPs  
719 (Table 3). The FCI index is an important indicator of changes in system functioning (Fath et  
720 al., 2019; Safi et al., 2019) and gives information about carbon cycling in the ecosystem (Finn,  
721 1976; Saint-Béat et al., 2018). This index can indicate the degree of maturity, resilience and  
722 stability of the ecosystem (Vasconcellos et al., 1997; Duan et al., 2009; Niquil et al., 2012).  
723 Recycling can indeed reduce the impact of stress on the ecosystem by acting as a buffer.  
724 Therefore, increased recycling can give better resilience and stability to the system (Saint-Béat  
725 et al., 2015). In addition, the APL index – which measures the retention capacity of the system  
726 (Fath et al., 2019b; Kay et al., 1989) – is expected to be high in systems with high degrees of  
727 flow diversity and cycling (Christensen, 1995; Thomas and Christian, 2001). Both indexes  
728 showed similar spatial evolution, i.e., lower values in S4 than in the other stations (Fig. 8 D, E),  
729 indicating that the herbivorous food web observed in S4 was less stable than the multivorous  
730 and microbial pathways observed in the others stations. This is in agreement with Legendre and  
731 Rassoulzadegan (1995) and Meddeb et al. (2019), who reported lower stability of the  
732 herbivorous food web in comparison to the microbial and multivorous ones. The highest values  
733 of FCI and APL coincided with the multivorous food web in S2 – the station most exposed to  
734 the source of disturbance in the Gulf – TCG (Fig. 1). Thus, the increase in recycling and flow



735 diversity seemed to endow the system with a certain resistance to the strong disturbance that  
736 the PTP underwent in S2. According to the MFA results, the APL seemed to be less structuring  
737 in the system since its contribution was not significant on the first two axes. In this case,  
738 considering the first two axes of the MFA, FCI seemed to be more efficient in the stability  
739 analysis.

740 The detritivory/herbivory ratio (D/H), which was initially adapted from Odum (1969),  
741 was applied to show the importance of detritivory compared to herbivory. Several authors have  
742 used this index to provide information on carbon transfer to consumers *via* detritus and/or  
743 autotrophs (Kay et al., 1989; Ulanowicz, 1992; Chrystal and Scharler, 2014; Niquil et al., 2014;  
744 Fath et al., 2019; Safi et al., 2019). High D/H values reflect an ecosystem where detritus plays  
745 an important role in carbon recycling, while low D/H values indicate an ecosystem where  
746 primary producers play a vital role as food for the second level (Chrystal and Scharler, 2014;  
747 Luong et al., 2014). During our study, the ratio indeed showed significant spatial variation  
748 (Table 3, Fig. 8 F), indicating a shift from systems based on the primary production pathway in  
749 S1 and S4 (D/H: 0.7 and 0.5, respectively) to systems based on phytoplankton and the detrital  
750 energy pathway, which played an important role in S2 and S3 (D/H ~ 1). This is consistent with  
751 the fact that R6 and R4 were similar in S2 and S3 (Fig. 7 A, B). Therefore, both phytoplankton  
752 and non-living carbon production played an important role for the multivorous food web  
753 observed in these stations. The lowest D/H value coincided with the herbivorous food web  
754 acting in the most eutrophic station S4. This is in agreement with the results of Luong et al.  
755 (2014), who reported that nutrient-rich environments favor herbivory over detritivory.

#### 756 **4.3. Importance of coupling ENA and typology ratios for ecosystem health** 757 **monitoring and management perspectives**

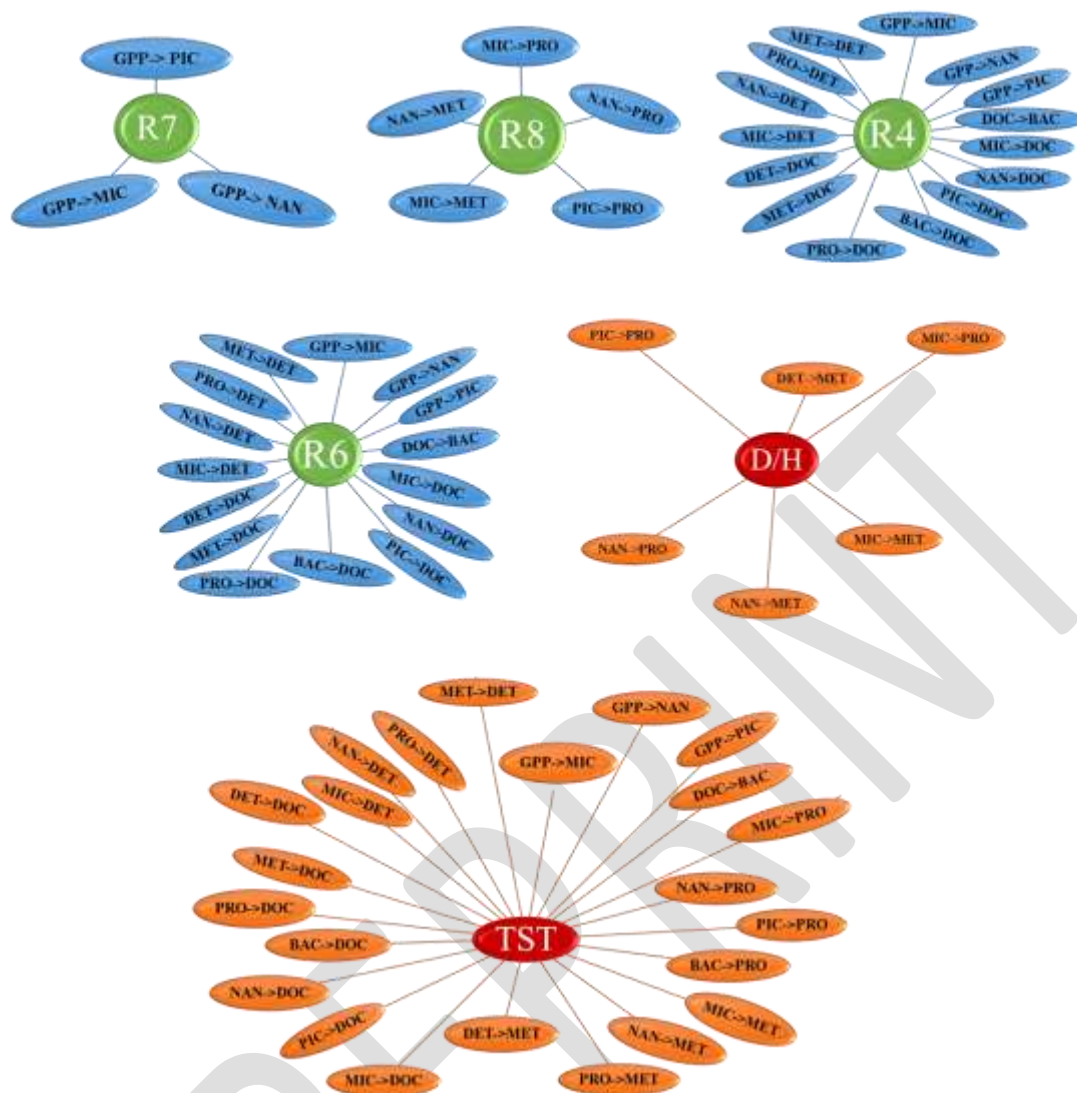
758 A representation of ecosystem dynamics based on the coupling of typology with ENA  
759 indicators may be considered as an effective tool for environmental managers. ENAs are  
760 sensitive tools for characterizing the ecosystem health status that have been repeatedly used to



761 assess the impact of natural and anthropogenic pressures on coastal marine ecosystems (Niquil  
762 et al., 2014; Pezy et al., 2017; Tecchio et al., 2016; de la Vega et al., 2018a, b; Safi et al., 2019;  
763 Fath et al., 2019). However, they can only partially capture the anthropogenic or natural stress  
764 levels of different types of food webs in aquatic ecosystems (Tecchio et al., 2016).

765 Thus, ecosystem models are increasingly used to advise water and marine policy makers  
766 in European Union countries (e.g. Heymans et al., 2020), but given the complexity of  
767 interactions within an ecosystem (Fath et al., 2007; Baird et al., 2009) and that model results  
768 represent projections of reality in a digital form, using and understanding these models is  
769 difficult for non-experts. Fath et al. (2019) recently reported that ENA indices are important,  
770 but currently difficult to understand for non-specialists and therefore difficult to use in  
771 communications. Typology ratios could be more practical for experts and non-experts alike.  
772 The advantage of these ratios is that if we consider some of them, we can directly access the  
773 specific fluxes without having to recur to modeling and calculate all the fluxes of the entire  
774 food web, as in the case of most ENA indices. For example, the identification of the dominant  
775 trophic pathway in a plankton assemblage could be based on these ratios, which can be  
776 calculated from flow values relatively easy to estimate in the field such as net  
777 picophytoplankton production divided by total phytoplankton production (R7), or the rate of  
778 consumption of total phytoplankton by protozooplankton divided by the rate of total  
779 consumption by proto- and metazooplankton (R8) (Fig. 10). Similarly, the material on which  
780 the system is based could be determined using criteria calculated from field-estimated fluxes,  
781 namely, total phytoplankton production divided by potential food production by  
782 protozooplankton (R4) or DOC and detritus production divided by potential food production  
783 by protozooplankton (R6) (Fig. 10) (Sakka Hlaili et al., 2014). This would facilitate decision-  
784 making about ecosystems. ENA results provide a better understanding of the functioning of the  
785 various structures of the planktonic food web under anthropogenic pressure, namely its activity  
786 (TST) and the importance of detritus in relation to phytoplankton production (D/H) in the  
787 system. Thus, from a planktonic perspective, these two indices often recommended by several

788 authors (Ulanowicz, 2004; Bodini et al., 2012; Fath et al., 2019; Safi et al., 2019) could also be  
789 easily estimated from field data (Fig. 10). They could be coupled with trophic typology ratios  
790 (R4, R6, R7 and R8) to better understand the functioning of different planktonic food web  
791 structures under anthropogenic pressure. In fact, the MFA carried out in this study showed that  
792 these ecological indicators (TST, D/H, R4, R6, R7 and R8) were the most structuring ones in  
793 the studied systems. Thus, the coupling of different indices could be more descriptive of food  
794 web functioning. For example, R4 and R6 indicate whether the system is based on non-living  
795 matter (DET, DOC) (low R4 and high R6) or instead on phytoplankton (low R4 and high R6)  
796 (Sakka Hlaili et al., 2014). The D/H index can be used in addition to these typology ratios to  
797 determine which of these two sources dominates (Fath et al., 2019). According to the MFA  
798 results (Fig. 9 A), the anti-correlation between D/H and R6 on the positive pole and R4 on the  
799 negative pole of axis 2 indeed reflects different ecosystems (Fig. 9 B). The high D/H values can  
800 be sustained by a higher R6 than R4, indicating that detritus play an important role in ecosystem  
801 recycling, e.g., carbon recycling. Conversely, low D/H values can be maintained by a higher  
802 R4 than R6, indicating an ecosystem where primary producers (phytoplankton and/or algae)  
803 play a substantial role as feed for consumers (PRO and MET) (Luong et al., 2014). R7, R8 and  
804 TST may be also complementary and interact in the description of the primary production of  
805 the planktonic food web type and its fate (Fig. 9). R7 provides information on the relative  
806 contribution of large and small phytoplankton to total primary production (Sakka Hlaili et al.,  
807 2014). Thus, it provides indirect information on the amount of primary production in the  
808 system, which may have an effect on the ecosystem activity measured by the TST (Finn, 1976;  
809 Ulanowicz, 1986; Borrett and Scharler, 2019). Moreover, we can refer to R8 to identify the  
810 main grazers of production. Grazers switch from MET (high R8) when herbivorous or  
811 multivorous food webs are dominant to PRO (low R8) when microbial pathways prevail (Sakka  
812 Hlaili et al., 2014).



813

814 **Fig.10.** Diagram illustrating the different flows involved in estimating the typology ratios (R4,  
815 R6, R7 and R8) and ENA indices (D/H, TST). The description of each flow is detailed in  
816 Table 2.

817 In general, although ENA indices faithfully characterize carbon circulation within  
818 planktonic food webs, they could be complemented with typological indices to make their  
819 interpretation easier and describe the main trophic pathways.

820 Despite efforts in the management of marine ecosystems, there are still gaps in the  
821 relationships between planktonic food web levels and benthic/pelagic organisms. The  
822 planktonic food web typology approach has only been partially addressed by managers. This is  
823 the first time that a local approach to a eutrophication gradient has been based on differences  
824 in PTP typology. The same approach is currently used by OSPAR to define MSFD D4

825 indicators, as stated in [Schückel et al. \(2022\)](#) (OSPAR quality report status validated for  
826 publication in September 2023). However, OSPAR uses complete models, where plankton is  
827 often represented in a rather incomplete way (for example, protozooplankton is not considered).

828 At the base of the pelagic food web, plankton and the existing fluxes of matter among  
829 planktonic compartments largely condition the functioning of the ecosystem because they are  
830 a source of primary production, are exported to the benthos or related ecosystems, and condition  
831 trophic efficiency towards the upper links ([Legendre and Rassoulzadegan, 1995](#); [Dupuy et al.,  
832 1999](#); [Sintes et al., 2004](#); [Leguerrier, 2005](#); [Marquis et al., 2007](#)). As a result, indices of the  
833 typology and functioning of the planktonic food web can be linked to the benthos and the higher  
834 trophic links from the export estimate. In addition, they can also give an idea of the emerging  
835 properties of the whole ecosystem (activity, export, recycling...).

836 The present study is based on a correlative approach, using MFA that links three levels:  
837 i) the nutrient gradient, ii) the type of RTP, and iii) the indicators that seemed best able to  
838 distinguish the four stations and their ecological functioning. On the basis of our conclusions,  
839 we can propose a new, original monitoring protocol that links typology ratios and ENA. Like  
840 ENA, ratios are based on food web flows, but they involve fewer flows, so that they can be  
841 estimated without necessarily quantifying the entire system. This approach differentiates ratios  
842 locally. Therefore, typology ratios appear as the best candidates for more operational  
843 development in the future.

844 Issues still remain to be solved. The first issue is that our study is local, so that our  
845 conclusions are not generic – further studies are needed for that –, but we do propose a protocol  
846 that can be applied to other sites to generalize our conclusions. This protocol should be tested  
847 in other cases of pollution (other than eutrophication) to determine the extent to which it is  
848 applicable and can be taken into account by managers. Another issue is that ecosystem  
849 management is in its formulation clearly intended to represent a complete food web (and  
850 therefore a complete ecosystem). Since typology ratios can be used to analyze planktonic food

851 webs (Sakka Hlaili et al., 2014), we now need to test them with ENAs in complete food webs,  
852 i.e. taking pelagic and benthic webs into account in the analyses.

## 853 5. Conclusion

854 The present study provides an analysis of the food web structure in the permanently  
855 disturbed Gulf of Gabès. An approach combining ecological network analysis (ENA) selected  
856 on the basis of previous literature and typology reports was tested. The study site was  
857 characterized by nutrient inputs (mainly from TCG), whose association with hydrodynamics  
858 has created a gradient of nutrient richness. The size structure of primary production, trophic  
859 interactions, the food web structure and function differed among the stations. The main results  
860 showed that:

861 ➤ The microbial food web dominated in the least nutrient-rich system S1. It was  
862 identified by the highest value of R7 and formed a phytoplankton-based food web ( $R4 > R6$ )  
863 primarily assigned to PRO (higher R8). PRO was inefficient in channeling biogenic carbon.  
864 This food web showed the lowest total system throughput (TST), and a low detritivory to  
865 herbivory (D/H) ratio, indicating a less active system relying on primary production  
866 (phytoplankton).

867 ➤ In contrast, the herbivorous food web indicated by the lowest value of R7 was  
868 identified in the most eutrophic system S4, where large phytoplankton dominated primary  
869 production ( $R4 > R6$ ) and were assigned to PRO and MET (lowest R8). These were efficiently  
870 exported to higher consumers. Thus, all ecological indicators were lowest in this food web,  
871 except TST that was highest. This indicates that the herbivorous food web of the system was  
872 more active based on primary production (low D/H) but less organized (low A/C) and less  
873 stable (low FCI).

874 ➤ The multivorous food web, as indicated by R7, dominated in the moderately  
875 nutrient-rich systems S2 and S3, and carbon production was based on both phytoplankton and  
876 non-living carbon ( $R4 \sim R6$ ) assigned to PRO and MET (low R8). These can be

877 efficient in carbon transfer. This food web was characterized by the highest relative  
878 ascendancy and cycling values (A/C and FCI), and was more organized, specialized and  
879 stable. It also showed a higher total system throughput and the highest D/H, reflecting a more  
880 active system where detritus play an important role in carbon recycling.

881 From an ecosystem management perspective, we propose a comprehensive assessment of  
882 ecosystem health based on appropriate indicators of food web typology and ENA indices, to be  
883 used by managers to assess the structure, functioning, and emerging properties of ecosystems  
884 under anthropogenic pressure. We suggest combining typology ratios to identify food web types  
885 with ENA indices to distinguish different food web functions across nutrient gradients. This  
886 combination can provide an effective tool for managing and assessing ecosystem health, and  
887 for investigating the occurrence of anthropogenic pressures.

## 888 **References:**

- 889  
890 Ayadi, N., Aloulou, F., Bouzid, J., 2015. Assessment of contaminated sediment by phosphate  
891 fertilizer industrial waste using pollution indices and statistical techniques in the Gulf  
892 of Gabes (Tunisia). *Arab J Geosci* 8, 1755–1767. <https://doi.org/10.1007/s12517-014-1291-4>  
893  
894 Ayata, S.-D., Irisson, J.-O., Aubert, A., Berline, L., Dutay, J.-C., Mayot, N., Nieblas, A.-E.,  
895 D'Ortenzio, F., Palmiéri, J., Reygondeau, G., Rossi, V., Guieu, C., 2018.  
896 Regionalisation of the Mediterranean basin, a MERMEX synthesis. *Progress in*  
897 *Oceanography*, Special issue of MERMEX project: Recent advances in the  
898 oceanography of the Mediterranean Sea 163, 7–20.  
899 <https://doi.org/10.1016/j.pocean.2017.09.016>  
900 Bagstad, K.J., Semmens, D.J., Waage, S., Winthrop, R., 2013. A comparative assessment of  
901 decision-support tools for ecosystem services quantification and valuation. *Ecosystem*  
902 *Services* 5, 27–39. <https://doi.org/10.1016/j.ecoser.2013.07.004>  
903 Baird, A.H., Guest, J.R., Willis, B.L., 2009. Systematic and biogeographical patterns in the  
904 reproductive biology of scleractinian corals. *Annual Review of Ecology, Evolution, and*  
905 *Systematics* 40, 551–571. <https://doi.org/10.1146/annurev.ecolsys.110308.120220>  
906 Béjaoui, B., Ben Ismail, S., Othmani, A., Ben Abdallah-Ben Hadj Hamida, O., Chevalier, C.,  
907 Feki-Sahnoun, W., Harzallah, A., Ben Hadj Hamida, N., Bouaziz, R., Dahech, S., Diaz,  
908 F., Tounsi, K., Sammari, C., Pagano, M., Bel Hassen, M., 2019. Synthesis review of the  
909 Gulf of Gabes (eastern Mediterranean Sea, Tunisia): Morphological, climatic, physical  
910 oceanographic, biogeochemical and fisheries features. *Estuarine, Coastal and Shelf*  
911 *Science* 219, 395–408. <https://doi.org/10.1016/j.ecss.2019.01.006>  
912 Bel Hassen, M., Drira, Z., Hamza, A., Ayadi, H., Akrouf, F., Issaoui, H., 2008. Summer  
913 phytoplankton pigments and community composition related to water mass properties  
914 in the Gulf of Gabes. *Estuarine, Coastal and Shelf Science* 77, 645–656.  
915 <https://doi.org/10.1016/j.ecss.2007.10.027>



- 916 Bel Hassen, M.B., Hamza, A., Drira, Z., Zouari, A., Akrouf, F., Messaoudi, S., Aleya, L., Ayadi,  
917 H., 2009. Phytoplankton-pigment signatures and their relationship to spring–summer  
918 stratification in the Gulf of Gabes. *Estuarine, Coastal and Shelf Science* 83, 296–306.  
919 <https://doi.org/10.1016/j.ecss.2009.04.002>
- 920 Belgrano, A., Scharler, S.E.R.C.U.M., Scharler, U.M., Dunne, J., Ulanowicz, R.E., 2005.  
921 *Aquatic Food Webs: An Ecosystem Approach*. OUP Oxford.
- 922 Bell, P.R.F., Elmetri, I., 1995. Ecological indicators of large-scale eutrophication in the Great  
923 Barrier Reef lagoon. *Oceanographic Literature Review* 12, 1145.
- 924 Bellinger, B.J., Cocquyt, C., O'Reilly, C.M., 2006. Benthic diatoms as indicators of  
925 eutrophication in tropical streams. *Hydrobiologia* 573, 75–87.  
926 <https://doi.org/10.1007/s10750-006-0262-5>
- 927 Ben Brahim, M., Hamza, A., Hannachi, I., Rebai, A., Jarboui, O., Bouain, A., Aleya, L., 2010.  
928 Variability in the structure of epiphytic assemblages of *Posidonia oceanica* in relation  
929 to human interferences in the Gulf of Gabes, Tunisia. *Marine Environmental Research*  
930 70, 411–421. <https://doi.org/10.1016/j.marenvres.2010.08.005>
- 931 Beske-Janssen, P., Johnson, M.P., Schaltegger, S., 2015. 20 years of performance measurement  
932 in sustainable supply chain management – what has been achieved? *Supply Chain*  
933 *Management: An International Journal* 20, 664–680. [https://doi.org/10.1108/SCM-06-](https://doi.org/10.1108/SCM-06-2015-0216)  
934 [2015-0216](https://doi.org/10.1108/SCM-06-2015-0216)
- 935 Bevilacqua, S., Airoidi, L., Ballesteros, E., Benedetti-Cecchi, L., Boero, F., Bulleri, F., Cebrian,  
936 E., Cerrano, C., Claudet, J., Colloca, F., Coppari, M., Di Franco, A., Frascchetti, S.,  
937 Garrabou, J., Guarnieri, G., Guerranti, C., Guidetti, P., Halpern, B.S., Katsanevakis, S.,  
938 Mangano, M.C., Micheli, F., Milazzo, M., Pusceddu, A., Renzi, M., Rilov, G., Sarà, G.,  
939 Terlizzi, A., 2021. Chapter One - Mediterranean rocky reefs in the Anthropocene:  
940 Present status and future concerns, in: Sheppard, C. (Ed.), *Advances in Marine Biology*.  
941 Academic Press, pp. 1–51. <https://doi.org/10.1016/bs.amb.2021.08.001>
- 942 Bodini, A., Bondavalli, C., Allesina, S., 2012a. Cities as ecosystems: Growth, development and  
943 implications for sustainability. *Ecological Modelling*, 7th European Conference on  
944 Ecological Modelling (ECEM) 245, 185–198.  
945 <https://doi.org/10.1016/j.ecolmodel.2012.02.022>
- 946 Bodini, A., Bondavalli, C., Allesina, S., 2012b. Cities as ecosystems: Growth, development and  
947 implications for sustainability. *Ecological Modelling*, 7th European Conference on  
948 Ecological Modelling (ECEM) 245, 185–198.  
949 <https://doi.org/10.1016/j.ecolmodel.2012.02.022>
- 950 Borrett, S.R., Scharler, U.M., 2019. Walk partitions of flow in Ecological Network Analysis:  
951 Review and synthesis of methods and indicators. *Ecological Indicators* 106, 105451.  
952 <https://doi.org/10.1016/j.ecolind.2019.105451>
- 953 Boudaya, L., Mosbahi, N., Dauvin, J.-C., Neifar, L., 2019. Structure of the benthic macrofauna  
954 of an anthropogenic influenced area: Skhira Bay (Gulf of Gabès, central Mediterranean  
955 Sea). *Environ Sci Pollut Res* 26, 13522–13538. [https://doi.org/10.1007/s11356-019-](https://doi.org/10.1007/s11356-019-04809-8)  
956 [04809-8](https://doi.org/10.1007/s11356-019-04809-8)
- 957 Cardoso, A., Cochrane, S., Doerner, H., Ferreira, J., Galgani, F., Hagebro, C., Hanke, G.,  
958 Hoepffner, N., Keizer, P., Law, R., Olenin, S., Piet, G., Rice, J., Rogers, S.,  
959 Swartenbroux, F., Tasker, M., Van, D.B.W., 2010. Scientific Support to the European  
960 Commission on the Marine Strategy Framework Directive - Management Group Report  
961 [WWW Document]. JRC Publications Repository. <https://doi.org/10.2788/86430>
- 962 Carpenter, S.R., Mooney, H.A., Agard, J., Capistrano, D., DeFries, R.S., Díaz, S., Dietz, T.,  
963 Duraiappah, A.K., Oteng-Yeboah, A., Pereira, H.M., Perrings, C., Reid, W.V.,  
964 Sarukhan, J., Scholes, R.J., Whyte, A., 2009. Science for managing ecosystem services:  
965 Beyond the Millennium Ecosystem Assessment. *Proc. Natl. Acad. Sci. U.S.A.* 106,  
966 1305–1312. <https://doi.org/10.1073/pnas.0808772106>
- 967 Chaalali, A., Saint-Béat, B., Lassalle, G., Le Loc'h, F., Tecchio, S., Safi, G., Savenkoff, C.,  
968 Lobry, J., Niquil, N., 2015. A new modeling approach to define marine ecosystems



- 969 food-web status with uncertainty assessment. *Progress in Oceanography* 135, 37–47.  
970 <https://doi.org/10.1016/j.pocean.2015.03.012>
- 971 Chaalali, A., Beaugrand, G., Raybaud, V., Lassalle, G., Saint-Béat, B., Le Loc'h, F., Bopp, L.,  
972 Tecchio, S., Safi, G., Chifflet, M., Lobry, J., Niquil, N., 2016. From species distributions  
973 to ecosystem structure and function: A methodological perspective. *Ecological*  
974 *Modelling* 334, 78–90. <https://doi.org/10.1016/j.ecolmodel.2016.04.022>
- 975 Chkili, O., Meddeb, M., Mejri Kousri, K., Melliti Ben Garali, S., Makhoulouf Belkhalia, N.,  
976 Tedetti, M., Pagano, M., Belaaj Zouari, A., Belhassen, M., Niquil, N., Sakka Hlaili, A.,  
977 2023. Influence of Nutrient Gradient on Phytoplankton Size Structure, Primary  
978 Production and Carbon Transfer Pathway in a Highly Productive Area (SE  
979 Mediterranean). *Ocean Sci. J.* 58, 6. <https://doi.org/10.1007/s12601-023-00101-6>
- 980 Christensen, V., 1995. Ecosystem maturity — towards quantification. *Ecological Modelling* 77,  
981 3–32. [https://doi.org/10.1016/0304-3800\(93\)E0073-C](https://doi.org/10.1016/0304-3800(93)E0073-C)
- 982 Christensen, V., Walters, C., Pauly, D., 2005. *Ecopath with Ecosim: A User's Guide*. Fisheries  
983 Centre, University of British Columbia, Vancouver, Canada and ICLARM, Penang,  
984 Malaysia 12.
- 985 Christian, R.R., Brinson, M.M., Dame, J.K., Johnson, G., Peterson, C.H., Baird, D., 2009.  
986 Ecological network analyses and their use for establishing reference domain in  
987 functional assessment of an estuary. *Ecological Modelling*, Special Issue on Cross-  
988 Disciplinary Informed Ecological Network Theory 220, 3113–3122.  
989 <https://doi.org/10.1016/j.ecolmodel.2009.07.012>
- 990 Chrystal, R.A., Scharler, U.M., 2014. Network analysis indices reflect extreme hydrodynamic  
991 conditions in a shallow estuarine lake (Lake St Lucia), South Africa. *Ecological*  
992 *Indicators* 38, 130–140. <https://doi.org/10.1016/j.ecolind.2013.10.025>
- 993 Coll, M., Santojanni, A., Palomera, I., Tudela, S., Arneri, E., 2007. An ecological model of the  
994 Northern and Central Adriatic Sea: Analysis of ecosystem structure and fishing impacts.  
995 *Journal of Marine Systems* 67, 119–154. <https://doi.org/10.1016/j.jmarsys.2006.10.002>
- 996 Corrales, X., Coll, M., Tecchio, S., Bellido, J.M., Fernández, Á.M., Palomera, I., 2015.  
997 Ecosystem structure and fishing impacts in the northwestern Mediterranean Sea using a  
998 food web model within a comparative approach. *Journal of Marine Systems* 148, 183–  
999 199. <https://doi.org/10.1016/j.jmarsys.2015.03.006>
- 1000 Danovaro, R., 2003. Pollution threats in the Mediterranean Sea: An Overview. *Chemistry and*  
1001 *Ecology - CHEM ECOL* 19, 15–32. <https://doi.org/10.1080/0275754031000081467>
- 1002 Danovaro, R., Fanelli, E., Aguzzi, J., Billett, D., Carugati, L., Corinaldesi, C., Dell'Anno, A.,  
1003 Gjerde, K., Jamieson, A.J., Kark, S., McClain, C., Levin, L., Levin, N., Ramirez-Llodra,  
1004 E., Ruhl, H., Smith, C.R., Snelgrove, P.V.R., Thomsen, L., Van Dover, C.L., Yasuhara,  
1005 M., 2020. Ecological variables for developing a global deep-ocean monitoring and  
1006 conservation strategy. *Nat Ecol Evol* 4, 181–192. <https://doi.org/10.1038/s41559-019-1091-z>
- 1007
- 1008 De Jonge, V.N., Schückel, U., 2021. A comprehensible short list of ecological network analysis  
1009 indices to boost real ecosystem-based management and policy making. *Ocean & Coastal*  
1010 *Management* 208, 105582. <https://doi.org/10.1016/j.ocecoaman.2021.105582>
- 1011 De la Vega, C., Horn, S., Baird, D., Hines, D., Borrett, S., Jensen, L.F., Schwemmer, P., Asmus,  
1012 R., Siebert, U., Asmus, H., 2018a. Seasonal dynamics and functioning of the Sylt-Rømø  
1013 Bight, northern Wadden Sea. *Estuarine, Coastal and Shelf Science* 203, 100–118.  
1014 <https://doi.org/10.1016/j.ecss.2018.01.021>
- 1015 De la Vega, C., Schückel, U., Horn, S., Kröncke, I., Asmus, R., Asmus, H., 2018b. How to  
1016 include ecological network analysis results in management? A case study of three tidal  
1017 basins of the Wadden Sea, south-eastern North Sea. *Ocean & Coastal Management* 163,  
1018 401–416. <https://doi.org/10.1016/j.ocecoaman.2018.07.019>
- 1019 De Laender, F., Van Oevelen, D., Soetaert, K., Middelburg, J., 2010. Carbon transfer in a  
1020 herbivore- and microbial loop-dominated pelagic food webs in the southern Barents Sea

- 1021 during spring and summer. *Mar. Ecol. Prog. Ser.* 398, 93–107.  
1022 <https://doi.org/10.3354/meps08335>
- 1023 Decembrini, F., Caroppo, C., Azzaro, M., 2009. Size structure and production of phytoplankton  
1024 community and carbon pathways channelling in the Southern Tyrrhenian Sea (Western  
1025 Mediterranean). *Deep Sea Research Part II: Topical Studies in Oceanography, Multi-*  
1026 *disciplinary forays into the south Tyrrhenian Sea - 2005 CIESM/SUB cruises 56*, 687–  
1027 699. <https://doi.org/10.1016/j.dsr2.2008.07.022>
- 1028 Decembrini, F., Caroppo, C., Caruso, G., Bergamasco, A., 2021. Linking Microbial  
1029 Functioning and Trophic Pathways to Ecological Status in a Coastal Mediterranean  
1030 Ecosystem. *Water* 13, 1325. <https://doi.org/10.3390/w13091325>
- 1031 DGPA, 2015. *Annuaire des statistiques des pêches en Tunisie*. Ministère de l'Agriculture,  
1032 Tunisie.
- 1033 Dokulil, M.T., Qian, K., 2021. Photosynthesis, carbon acquisition and primary productivity of  
1034 phytoplankton: a review dedicated to Colin Reynolds. *Hydrobiologia* 848, 77–94.  
1035 <https://doi.org/10.1007/s10750-020-04321-y>
- 1036 D'Ortenzio, F., Ribera d'Alcalà, M., 2009. On the trophic regimes of the Mediterranean Sea: a  
1037 satellite analysis. *Biogeosciences* 6, 139–148. <https://doi.org/10.5194/bg-6-139-2009>
- 1038 Drira, Z., Hassen, M.B., Hamza, A., Rebai, A., Bouain, A., Ayadi, H., Aleya, L., 2009. Spatial  
1039 and temporal variations of microphytoplankton composition related to hydrographic  
1040 conditions in the Gulf of Gabès. *Journal of the Marine Biological Association of the*  
1041 *United Kingdom* 89, 1559–1569. <https://doi.org/10.1017/S002531540900023X>
- 1042 Drira, Z., Kmiha-Megdiche, S., Sahnoun, H., Tedetti, M., Pagano, M., Ayadi, H., 2018.  
1043 Copepod assemblages as a bioindicator of environmental quality in three coastal areas  
1044 under contrasted anthropogenic inputs (Gulf of Gabes, Tunisia). *Journal of the Marine*  
1045 *Biological Association of the United Kingdom* 98, 1889–1905.  
1046 <https://doi.org/10.1017/S0025315417001515>
- 1047 Duan, L.J., Li, S.Y., Liu, Y., Moreau, J., Christensen, V., 2009. Modeling changes in the coastal  
1048 ecosystem of the Pearl River Estuary from 1981 to 1998. *Ecological Modelling* 220,  
1049 2802–2818. <https://doi.org/10.1016/j.ecolmodel.2009.07.016>
- 1050 Dupuy, C., Gall, S.L., Hartmann, H.J., Bréret, M., 1999. Retention of ciliates and flagellates by  
1051 the oyster *Crassostrea gigas* in French Atlantic coastal ponds: protists as a trophic link  
1052 between bacterioplankton and benthic suspension-feeders. *Marine Ecology Progress*  
1053 *Series* 177, 165–175. <https://doi.org/10.3354/meps177165>
- 1054 Durrieu de Madron, X., Guieu, C., Sempéré, R., Conan, P., Cossa, D., D'Ortenzio, F.,  
1055 Estournel, C., Gazeau, F., Rabouille, C., Stemmann, L., Bonnet, S., Diaz, F., Koubbi,  
1056 P., Radakovitch, O., Babin, M., Baklouti, M., Bancon-Montigny, C., Belviso, S.,  
1057 Bensoussan, N., Bonsang, B., Bouloubassi, I., Brunet, C., Cadiou, J.-F., Carlotti, F.,  
1058 Chami, M., Charmasson, S., Charrière, B., Dachs, J., Doxaran, D., Dutay, J.-C., Elbaz-  
1059 Poulichet, F., Eléaume, M., Eyrolles, F., Fernandez, C., Fowler, S., Francour, P.,  
1060 Gaertner, J.C., Galzin, R., Gasparini, S., Ghiglione, J.-F., Gonzalez, J.-L., Goyet, C.,  
1061 Guidi, L., Guizien, K., Heimbürger, L.-E., Jacquet, S.H.M., Jeffrey, W.H., Joux, F., Le  
1062 Hir, P., Leblanc, K., Lefèvre, D., Lejeusne, C., Lemé, R., Loje-Pilot, M.-D., Mallet, M.,  
1063 Méjanelle, L., Mélin, F., Mellon, C., Mérigot, B., Merle, P.-L., Migon, C., Miller, W.L.,  
1064 Mortier, L., Mostajir, B., Mousseau, L., Moutin, T., Para, J., Pérez, T., Petrenko, A.,  
1065 Poggiale, J.-C., Prieur, L., Pujo-Pay, M., Pulido-Villena, Raimbault, P., Rees, A.P.,  
1066 Ridame, C., Rontani, J.-F., Ruiz Pino, D., Sicre, M.A., Taillandier, V., Tamburini, C.,  
1067 Tanaka, T., Taupier-Letage, I., Tedetti, M., Testor, P., Thébault, H., Thouvenin, B.,  
1068 Touratier, F., Tronczynski, J., Ulses, C., Van Wambeke, F., Vantrepotte, V., Vaz, S.,  
1069 Verney, R., 2011. Marine ecosystems' responses to climatic and anthropogenic forcings  
1070 in the Mediterranean. *Progress in Oceanography* 91, 97–166.  
1071 <https://doi.org/10.1016/j.pcean.2011.02.003>

- 1072 El Zrelli, R., Courjault-Radé, P., Rabaoui, L., Castet, S., Michel, S., Bejaoui, N., 2015. Heavy  
1073 metal contamination and ecological risk assessment in the surface sediments of the  
1074 coastal area surrounding the industrial complex of Gabes city, Gulf of Gabes, SE  
1075 Tunisia. *Marine Pollution Bulletin* 101, 922–929.  
1076 <https://doi.org/10.1016/j.marpolbul.2015.10.047>
- 1077 Enajjar, S., Saïdi, B., Bradai, M., 2015. The Gulf of Gabès (Central Mediterranean Sea): a  
1078 nursery area for sharks and batoids (Chondrichthyes: Elasmobranchs). *Cahiers de*  
1079 *Biologie Marine* 56, 143–150.
- 1080 Escofier, B., Pagès, J., 1990. *Analyses factorielles simples et multiples : objectifs, méthodes et*  
1081 *interprétation*. Dunod.
- 1082 European Commission, 2010. Commission Decision of 1 September 2010 on criteria and  
1083 methodological standards on good environmental status of marine waters (notified  
1084 under document C(2010) 5956) (Text with EEA relevance) (2010/477/EU).  
1085 <https://doi.org/10.25607/OBP-820>
- 1086 Fath, B.D., Asmus, H., Asmus, R., Baird, D., Borrett, S.R., de Jonge, V.N., Ludovisi, A., Niquil,  
1087 N., Scharler, U.M., Schüchel, U., Wolff, M., 2019. Ecological network analysis metrics:  
1088 The need for an entire ecosystem approach in management and policy. *Ocean & Coastal*  
1089 *Management* 174, 1–14. <https://doi.org/10.1016/j.ocecoaman.2019.03.007>
- 1090 Fath, B.D., Scharler, U.M., Ulanowicz, R.E., Hannon, B., 2007. Ecological network analysis:  
1091 network construction. *Ecological Modelling, Special Issue on Ecological Network*  
1092 *Theory* 208, 49–55. <https://doi.org/10.1016/j.ecolmodel.2007.04.029>
- 1093 Fath, B.D., Patten, B.C., 1999. Review of the Foundations of Network Environ Analysis.  
1094 *Ecosystems* 2, 167–179. <https://doi.org/10.1007/s100219900067>
- 1095 Filiz, N., Işkın, U., Beklioğlu, M., Öglü, B., Cao, Y., Davidson, T.A., Søndergaard, M.,  
1096 Lauridsen, T.L., Jeppesen, E., 2020. Phytoplankton Community Response to Nutrients,  
1097 Temperatures, and a Heat Wave in Shallow Lakes: An Experimental Approach. *Water*  
1098 12, 3394. <https://doi.org/10.3390/w12123394>
- 1099 Finn, J.T., 1976. Measures of ecosystem structure and function derived from analysis of flows.  
1100 *Journal of Theoretical Biology* 56, 363–380. [https://doi.org/10.1016/S0022-5193\(76\)80080-X](https://doi.org/10.1016/S0022-5193(76)80080-X)
- 1102 Fortier, L., Le Fèvre, J., Legendre, L., 1994. Export of biogenic carbon to fish and to the deep  
1103 ocean: the role of large planktonic microphages. *Journal of Plankton Research* 16, 809–  
1104 839. <https://doi.org/10.1093/plankt/16.7.809>
- 1105 Froneman, P.W., 2004. Food web dynamics in a temperate temporarily open/closed estuary  
1106 (South Africa). *Estuarine, Coastal and Shelf Science* 59, 87–95.  
1107 <https://doi.org/10.1016/j.ecss.2003.08.003>
- 1108 Gaichas, S.K., 2008. A context for ecosystem-based fishery management: Developing concepts  
1109 of ecosystems and sustainability. *Marine Policy* 32, 393–401.  
1110 <https://doi.org/10.1016/j.marpol.2007.08.002>
- 1111 Goldman, J., Caron, D., Dennett, M., 1987. Nutrient cycling in a microflagellate food chain:  
1112 IV. Phytoplankton-microflagellate interactions. *Mar. Ecol. Prog. Ser.* 38, 75–87.  
1113 <https://doi.org/10.3354/meps038075>
- 1114 Gotwals, A.W., Songer, N.B., 2010. Reasoning up and down a food chain: Using an assessment  
1115 framework to investigate students' middle knowledge. *Science Education* 94, 259–281.  
1116 <https://doi.org/10.1002/sce.20368>
- 1117 Garmendia, M., Borja, Á., Franco, J., Revilla, M., 2013. Phytoplankton composition indicators  
1118 for the assessment of eutrophication in marine waters: Present state and challenges within  
1119 the European directives. *Marine Pollution Bulletin* 66, 7–16.  
1120 <https://doi.org/10.1016/j.marpolbul.2012.10.005>
- 1121 Grami, B., Niquil, N., Sakka Hlaili, A., Gosselin, M., Hamel, D., Hadj Mabrouk, H., 2008. The  
1122 plankton food web of the Bizerte Lagoon (South-western Mediterranean): II. Carbon

- 1123 steady-state modelling using inverse analysis. *Estuarine, Coastal and Shelf Science* 79,  
1124 101–113. <https://doi.org/10.1016/j.ecss.2008.03.009>
- 1125 Grami, B., Rasconi, S., Niquil, N., Jobard, M., Saint-Béat, B., Sime-Ngando, T., 2011.  
1126 Functional Effects of Parasites on Food Web Properties during the Spring Diatom  
1127 Bloom in Lake Pavin: A Linear Inverse Modeling Analysis. *PLOS ONE* 6, e23273.  
1128 <https://doi.org/10.1371/journal.pone.0023273>
- 1129 Haraldsson, M., Gerphagnon, M., Bazin, P., Colombet, J., Tecchio, S., Sime-Ngando, T.,  
1130 Niquil, N., 2018. Microbial parasites make cyanobacteria blooms less of a trophic dead  
1131 end than commonly assumed. *ISME J* 12, 1008–1020. [https://doi.org/10.1038/s41396-](https://doi.org/10.1038/s41396-018-0045-9)  
1132 [018-0045-9](https://doi.org/10.1038/s41396-018-0045-9)
- 1133 Hardikar, R., C.k., H., Ram, A., Parthipan, V., 2021. Distribution of size-fractionated  
1134 phytoplankton biomass from the anthropogenically stressed tropical creek (Thane creek,  
1135 India). *Regional Studies in Marine Science* 41, 101577.  
1136 <https://doi.org/10.1016/j.rsma.2020.101577>
- 1137 Hattour, M.J., Sammari, C., Ben Nassrallah, S., 2010. Hydrodynamique du golfe de Gabès  
1138 déduite à partir des observations de courants et de niveaux. *Revue Paralia* 3, 3.1-3.12.  
1139 <https://doi.org/10.5150/revue-paralia.2010.003>
- 1140 Heymans, J.J., Coll, M., Libralato, S., Morissette, L., Christensen, V., 2014. Global Patterns in  
1141 Ecological Indicators of Marine Food Webs: A Modelling Approach. *PLOS ONE* 9,  
1142 e95845. <https://doi.org/10.1371/journal.pone.0095845>
- 1143 Heymans, S.J.J., Skogen, M., Schrum, C., Solidoro, C., 2019. Enhancing Europe's capability  
1144 in end-to-end marine ecosystem modelling for societal benefit.  
1145 <https://doi.org/10.31230/osf.io/jhqvu>
- 1146 Hill, S.L., Murphy, E.J., Reid, K., Trathan, P.N., Constable, A.J., 2006. Modelling Southern  
1147 Ocean ecosystems: krill, the food-web, and the impacts of harvesting. *Biological*  
1148 *Reviews* 81, 581–608. <https://doi.org/10.1017/S1464793106007123>
- 1149 Hines, D.E., Ray, S., Borrett, S.R., 2018. Uncertainty analyses for Ecological Network Analysis  
1150 enable stronger inferences. *Environmental Modelling & Software* 101, 117–127.  
1151 <https://doi.org/10.1016/j.envsoft.2017.12.011>
- 1152 Horňák, K., Mašín, M., Jezbera, J., Bettarel, Y., Nedoma, J., Sime-Ngando, T., Šimek, K.,  
1153 2005. Effects of decreased resource availability, protozoan grazing and viral impact on  
1154 a structure of bacterioplankton assemblage in a canyon-shaped reservoir. *FEMS*  
1155 *Microbiology Ecology* 52, 315–327. <https://doi.org/10.1016/j.femsec.2004.11.013>
- 1156 Jørgensen, S.E., Patten, B.C., Straškraba, M., 2000. Ecosystems emerging:: 4. growth.  
1157 *Ecological Modelling* 126, 249–284. [https://doi.org/10.1016/S0304-3800\(00\)00268-4](https://doi.org/10.1016/S0304-3800(00)00268-4)
- 1158 Kay, J.J., Graham, L.A., Ulanowicz, R.E., 1989. A Detailed Guide to Network Analysis, in:  
1159 Wulff, F., Field, J.G., Mann, K.H. (Eds.), *Network Analysis in Marine Ecology*.  
1160 Springer Berlin Heidelberg, Berlin, Heidelberg, pp. 15–61. [https://doi.org/10.1007/978-](https://doi.org/10.1007/978-3-642-75017-5_2)  
1161 [3-642-75017-5\\_2](https://doi.org/10.1007/978-3-642-75017-5_2)
- 1162 Khammeri, Y., Bellaaj-Zouari, A., Hamza, A., Medhioub, W., Sahli, E., Akrouf, F., Barraaj, N.,  
1163 Ben Kacem, M.Y., Bel Hassen, M., 2020. Ultraphytoplankton community composition  
1164 in Southwestern and Eastern Mediterranean Basin: Relationships to water mass  
1165 properties and nutrients. *Journal of Sea Research* 158, 101875.  
1166 <https://doi.org/10.1016/j.seares.2020.101875>
- 1167 Khammeri, Y., Hamza, I.S., Zouari, A.B., Hamza, A., Sahli, E., Akrouf, F., Ben Kacem, M.Y.,  
1168 Messaoudi, S., Hassen, M.B., 2018. Atmospheric bulk deposition of dissolved nitrogen,  
1169 phosphorus and silicate in the Gulf of Gabès (South Ionian Basin); implications for  
1170 marine heterotrophic prokaryotes and ultraphytoplankton. *Continental Shelf Research*  
1171 159, 1–11. <https://doi.org/10.1016/j.csr.2018.03.003>
- 1172 Kiørboe, T., Hansen, J.L.S., Alldredge, A.L., Jackson, G.A., Passow, U., Dam, H.G., Drapeau,  
1173 D.T., Waite, A., Garcia, C.M., 1996. Sedimentation of phytoplankton during a diatom  
1174 bloom : Rates and mechanisms. *Journal of Marine Research* 54, 1123–1148.



- 1175 Kmiha-Megdiche, S., Rekik, A., Pagano, M., Ayadi, H., Elloumi, J., 2021. The influence of  
1176 environmental characteristics on the distribution of ciliates in two coastal areas in the  
1177 Eastern Mediterranean Sea (Gulf of Gabes, Tunisia). *Regional Studies in Marine*  
1178 *Science* 45, 101799. <https://doi.org/10.1016/j.rsma.2021.101799>
- 1179 Knights, A.M., Koss, R.S., Robinson, L.A., 2013. Identifying common pressure pathways from  
1180 a complex network of human activities to support ecosystem-based management.  
1181 *Ecological Applications* 23, 755–765. <https://doi.org/10.1890/12-1137.1>
- 1182 Koched, W.K., Alemany, F., Ismail, S.B., Benmessaoud, R., Hattour, A., Garcia, A., 2015.  
1183 Environmental conditions influencing the larval fish assemblage during summer in the  
1184 Gulf of Gabes (Tunisia: South central Mediterranean). *Mediterranean Marine Science*  
1185 16, 666–681. <https://doi.org/10.12681/mms.1158>
- 1186 Landry, M.R., Hassett, R.P., 1982. Estimating the grazing impact of marine micro-zooplankton.  
1187 *Marine Biology* 67, 283–288. <https://doi.org/10.1007/BF00397668>
- 1188 Latham, L.G., 2006. Network flow analysis algorithms. *Ecological Modelling* 192, 586–600.  
1189 <https://doi.org/10.1016/j.ecolmodel.2005.07.029>
- 1190 Latham, L.G., Scully, E.P., 2002. Quantifying constraint to assess development in ecological  
1191 networks. *Ecological Modelling* 154, 25–44. [https://doi.org/10.1016/S0304-](https://doi.org/10.1016/S0304-3800(02)00032-7)  
1192 [3800\(02\)00032-7](https://doi.org/10.1016/S0304-3800(02)00032-7)
- 1193 Legendre and Le Fèvre, L., 1989. Hydrodynamical singularities as controls of recycled versus  
1194 export production in oceans. *Productivity of the Ocean : Present and Pasts*.
- 1195 Legendre, L., Rassoulzadegan, F., 1996. Food-web mediated export of biogenic carbon in  
1196 oceans:hydrodynamic control. *Mar. Ecol. Prog. Ser.* 145, 179–193.  
1197 <https://doi.org/10.3354/meps145179>
- 1198 Legendre, L., Rassoulzadegan, F., 1995. Plankton and nutrient dynamics in marine waters.  
1199 *Ophelia* 41, 153–172. <https://doi.org/10.1080/00785236.1995.10422042>
- 1200 Leguerrier, D., 2005. Construction et étude d'un modèle de réseau trophique de la vasière de  
1201 Brouage (bassin de marennes Oléron, France). *Prise en compte de la saisonnalité et des*  
1202 *échanges physiques pour la synthèse constructive des connaissances sur une zone*  
1203 *intertidale d'une région tempérée*. Université de la Rochelle.
- 1204 Lewis, K.A., Christian, R.R., Martin, C.W., Allen, K.L., McDonald, A.M., Roberts, V.M.,  
1205 Shaffer, M.N., Valentine, J.F., 2022. Complexities of disturbance response in a marine  
1206 food web. *Limnology & Oceanography* 67. <https://doi.org/10.1002/lno.11790>
- 1207 Liqueste, C., Piroddi, C., Macías, D., Druon, J.-N., Zulian, G., 2016. Ecosystem services  
1208 sustainability in the Mediterranean Sea: assessment of status and trends using multiple  
1209 modelling approaches. *Sci Rep* 6, 34162. <https://doi.org/10.1038/srep34162>
- 1210 López-Abbate, M.C., Molinero, J.C., Barría de Cao, M.S., Silva, R., Negri, R., Guinder, V.A.,  
1211 Hozbor, M.C., Hoffmeyer, M.S., 2019. Eutrophication disrupts summer trophic links in  
1212 an estuarine microbial food web. *Food Webs* 20, e00121.  
1213 <https://doi.org/10.1016/j.fooweb.2019.e00121>
- 1214 Luong, A.D., De Laender, F., Olsen, Y., Vadstein, O., Dewulf, J., Janssen, C.R., 2014. Inferring  
1215 time-variable effects of nutrient enrichment on marine ecosystems using inverse  
1216 modelling and ecological network analysis. *Science of The Total Environment* 493,  
1217 708–718. <https://doi.org/10.1016/j.scitotenv.2014.06.027>
- 1218 Machado, K.B., Bini, L.M., Melo, A.S., Andrade, A.T. de, Almeida, M.F. de, Carvalho, P.,  
1219 Teresa, F.B., Roque, F. de O., Bortolini, J.C., Padial, A.A., Vieira, L.C.G., Dala-Corte,  
1220 R.B., Siqueira, T., Juen, L., Dias, M.S., Gama Júnior, W.A., Martins, R.T., Nabout, J.C.,  
1221 2023. Functional and taxonomic diversities are better early indicators of eutrophication  
1222 than composition of freshwater phytoplankton. *Hydrobiologia* 850, 1393–1411.  
1223 <https://doi.org/10.1007/s10750-022-04954-1>
- 1224 Marquis, E., Niquil, N., Delmas, D., Hartmann, H.J., Bonnet, D., Carlotti, F., Herbland, A.,  
1225 Labry, C., Sautour, B., Laborde, P., Vézina, A., Dupuy, C., 2007. Inverse analysis of  
1226 the planktonic food web dynamics related to phytoplankton bloom development on the

- 1227 continental shelf of the Bay of Biscay, French coast. *Estuarine, Coastal and Shelf*  
1228 *Science* 73, 223–235. <https://doi.org/10.1016/j.ecss.2007.01.003>
- 1229 Meddeb, M., Grami, B., Chaalali, A., Haraldsson, M., Niquil, N., Pringault, O., Sakka Hlaili,  
1230 A., 2018. Plankton food-web functioning in anthropogenically impacted coastal waters  
1231 (SW Mediterranean Sea): An ecological network analysis. *Progress in Oceanography*  
1232 162, 66–82. <https://doi.org/10.1016/j.pocean.2018.02.013>
- 1233 Meddeb, M., Niquil, N., Grami, B., Mejri, K., Haraldsson, M., Chaalali, A., Pringault, O.,  
1234 Hlaili, A.S., 2019. A new type of plankton food web functioning in coastal waters  
1235 revealed by coupling Monte Carlo Markov chain linear inverse method and ecological  
1236 network analysis. *Ecological Indicators* 104, 67–85.  
1237 <https://doi.org/10.1016/j.ecolind.2019.04.077>
- 1238 Meersche, K.V. den, Soetaert, K., Oevelen, D.V., 2009. xsample(): An R Function for Sampling  
1239 Linear Inverse Problems. *Journal of Statistical Software* 30, 1–15.  
1240 <https://doi.org/10.18637/jss.v030.c01>
- 1241 Méndez, M., García, D., Maestre, F.T., Escudero, A., 2008. More Ecology is Needed to Restore  
1242 Mediterranean Ecosystems: A Reply to Valladares and Gianoli. *Restoration Ecology*  
1243 16, 210–216. <https://doi.org/10.1111/j.1526-100X.2008.00390.x>
- 1244 Michel, C., Nielsen, T.G., Nozais, C., Gosselin, M., 2002. Significance of sedimentation and  
1245 grazing by ice micro- and meiofauna for carbon cycling in annual sea ice (northern  
1246 Baffin Bay). *Aquatic Microbial Ecology* 30, 57–68. <https://doi.org/10.3354/ame030057>
- 1247 Mousseau, L., Klein, B., Legendre, L., Dauchez, S., Tamigneaux, E., Tremblay, J.-E., Ingram,  
1248 R.G., 2001. Assessing the trophic pathways that dominate planktonic food webs: an  
1249 approach based on simple ecological ratios. *Journal of Plankton Research* 23, 765–777.  
1250 <https://doi.org/10.1093/plankt/23.8.765>
- 1251 Niquil, N., Baeta, A., Marques, J.C., Chaalali, A., Lobry, J., Patrício, J., 2014a. Reaction of an  
1252 estuarine food web to disturbance: Lindeman’s perspective. *Marine Ecology Progress*  
1253 *Series* 512, 141–154. <https://doi.org/10.3354/meps10885>
- 1254 Niquil, N., Baeta, A., Marques, J.C., Chaalali, A., Lobry, J., Patrício, J., 2014b. Reaction of an  
1255 estuarine food web to disturbance: Lindeman’s perspective. *Marine Ecology Progress*  
1256 *Series* 512, 141–154. <https://doi.org/10.3354/meps10885>
- 1257 Niquil, N., Chaumillon, E., Johnson, G.A., Bertin, X., Grami, B., David, V., Bacher, C., Asmus,  
1258 H., Baird, D., Asmus, R., 2012. The effect of physical drivers on ecosystem indices  
1259 derived from ecological network analysis: Comparison across estuarine ecosystems.  
1260 *Estuarine, Coastal and Shelf Science*, ECSA 46 Conference Proceedings 108, 132–143.  
1261 <https://doi.org/10.1016/j.ecss.2011.12.031>
- 1262 Niquil, N., Soetaert, K.E.R., Johnson, G.A., Van Oevelen, D., Bacher, C., Saint-Béat, B.,  
1263 Vézina, A.F., 2011. Inverse modelling in modern ecology and application to coastal  
1264 ecosystems, in: Wolanski, E., Mclusky, D. (Eds.), *Estuarine and Coastal Ecosystem*  
1265 *Modelling*, Treatise on Estuarine and Coastal Science. Elsevier B.V., pp. 115–133.  
1266 <https://doi.org/10.1016/B978-0-12-374711-2.00906-2>
- 1267 Nogues, Q., Raoux, A., Aраignous, E., Chaalali, A., Hattab, T., Leroy, B., Ben Rais Lasram, F.,  
1268 David, V., Le Loc’h, F., Dauvin, J.-C., Niquil, N., 2021. Cumulative effects of marine  
1269 renewable energy and climate change on ecosystem properties: Sensitivity of ecological  
1270 network analysis. *Ecological Indicators* 121, 107128.  
1271 <https://doi.org/10.1016/j.ecolind.2020.107128>
- 1272 Odum, E.P., 1969. The Strategy of Ecosystem Development. *Science* 164, 262–270.  
1273 <https://doi.org/10.1126/science.164.3877.262>
- 1274 Othmani, A., Béjaoui, B., Chevalier, C., Elhmaidi, D., Devenon, J.-L., Aleya, L., 2017. High-  
1275 resolution numerical modelling of the barotropic tides in the Gulf of Gabes, eastern  
1276 Mediterranean Sea (Tunisia). *Journal of African Earth Sciences* 129, 224–232.  
1277 <https://doi.org/10.1016/j.jafrearsci.2017.01.007>
- 1278 Pacella, S.R., Lebreton, B., Richard, P., Phillips, D., DeWitt, T.H., Niquil, N., 2013.  
1279 Incorporation of diet information derived from Bayesian stable isotope mixing models



- 1280 into mass-balanced marine ecosystem models: A case study from the Marennes-Oléron  
1281 Estuary, France. *Ecological Modelling* 267, 127–137.  
1282 <https://doi.org/10.1016/j.ecolmodel.2013.07.018>
- 1283 Parsons, P.J.Harrison, Author links open overlay  
1284 panel T.R.Parsons\*P.J.Harrison\*J.C.Acreman\*H.M.Dovey\*P.A.Thompson\*C.M.Lalli  
1285 †K.LeeLiGuanguo, 1984. An experimental marine ecosystem response to crude oil and  
1286 Corexit 9527: Part 2—Biological effects - ScienceDirect [WWW Document]. URL  
1287 <https://www.sciencedirect.com/science/article/abs/pii/0141113684900333> (accessed  
1288 6.8.22).
- 1289 Patrício, J., Ulanowicz, R., Pardal, M.A., Marques, J.C., 2004. Ascendency as an ecological  
1290 indicator: a case study of estuarine pulse eutrophication. *Estuarine, Coastal and Shelf  
1291 Science* 60, 23–35. <https://doi.org/10.1016/j.ecss.2003.11.017>
- 1292 Pauly, D., Christensen, V., Walters, C., 2000. Ecopath, Ecosim, and Ecospace as tools for  
1293 evaluating ecosystem impact of fisheries. *ICES Journal of Marine Science* 57, 697–706.  
1294 <https://doi.org/10.1006/jmsc.2000.0726>
- 1295 Pezy, J.-P., Raoux, A., Marmin, S., Balay, P., Niquil, N., Dauvin, J.-C., 2017. Before-After  
1296 analysis of the trophic network of an experimental dumping site in the eastern part of  
1297 the Bay of Seine (English Channel). *Marine Pollution Bulletin* 118, 101–111.  
1298 <https://doi.org/10.1016/j.marpolbul.2017.02.042>
- 1299 Piroddi, C., Coll, M., Steenbeek, J., Macias Moy, D., Christensen, V., 2015. Modelling the  
1300 Mediterranean marine ecosystem as a whole: addressing the challenge of complexity.  
1301 *Mar. Ecol. Prog. Ser.* 533, 47–65. <https://doi.org/10.3354/meps11387>
- 1302 Raimbault, P., Garcia, N., Cerutti, F., 2008. Distribution of inorganic and organic nutrients in  
1303 the South Pacific Ocean & minus; evidence for long-term accumulation of organic  
1304 matter in nitrogen-depleted waters. *Biogeosciences* 5, 281–298.  
1305 <https://doi.org/10.5194/bg-5-281-2008>
- 1306 Reygondeau, G., Guieu, C., Benedetti, F., Irisson, J.-O., Ayata, S.-D., Gasparini, S., Koubbi,  
1307 P., 2017. Biogeochemical regions of the Mediterranean Sea: An objective  
1308 multidimensional and multivariate environmental approach. *Progress in Oceanography*  
1309 151, 138–148. <https://doi.org/10.1016/j.pocean.2016.11.001>
- 1310 Richardson, T.L., Jackson, G.A., 2007. Small Phytoplankton and Carbon Export from the  
1311 Surface Ocean. *Science* 315, 838–840. <https://doi.org/10.1126/science.1133471>
- 1312 Romano, J., Kromrey, J., Coraggio, J., 2006. Exploring methods for evaluating group  
1313 differences on the NSSE and other surveys: Are the t-test and Cohen’s d indices the  
1314 most appropriate choices? In annual meeting of the Southern Association for  
1315 Institutional Research 1–51.
- 1316 Rutledge, R.W., Basore, B.L., Mulholland, R.J., 1976. Ecological stability: An information  
1317 theory viewpoint. *Journal of Theoretical Biology* 57, 355–371.  
1318 [https://doi.org/10.1016/0022-5193\(76\)90007-2](https://doi.org/10.1016/0022-5193(76)90007-2)
- 1319 Safi, G., Giebels, D., Arroyo, N.L., Heymans, J.J., Preciado, I., Raoux, A., Schückel, U.,  
1320 Tecchio, S., de Jonge, V.N., Niquil, N., 2019. Vitamine ENA: A framework for the  
1321 development of ecosystem-based indicators for decision makers. *Ocean & Coastal  
1322 Management* 174, 116–130. <https://doi.org/10.1016/j.ocecoaman.2019.03.005>
- 1323 Saint-Béat, B., Baird, D., Asmus, H., Asmus, R., Bacher, C., Pacella, S.R., Johnson, G.A.,  
1324 David, V., Vézina, A.F., Niquil, N., 2015. Trophic networks: How do theories link  
1325 ecosystem structure and functioning to stability properties? A review. *Ecological  
1326 Indicators* 52, 458–471. <https://doi.org/10.1016/j.ecolind.2014.12.017>
- 1327 Saint-Béat, B., Dupuy, C., Bocher, P., Chalumeau, J., Crignis, M.D., Fontaine, C., Guizien, K.,  
1328 Lavaud, J., Lefebvre, S., Montanié, H., Mouget, J.-L., Orvain, F., Pascal, P.-Y.,  
1329 Quaintenne, G., Radenac, G., Richard, P., Robin, F., Vézina, A.F., Niquil, N., 2013.  
1330 Key Features of Intertidal Food Webs That Support Migratory Shorebirds. *PLOS ONE*  
1331 8, e76739. <https://doi.org/10.1371/journal.pone.0076739>

- 1332 Saint-Béat, B., Maps, F., Babin, M., 2018. Unraveling the intricate dynamics of planktonic  
1333 Arctic marine food webs. A sensitivity analysis of a well-documented food web model.  
1334 Progress in Oceanography 160, 167–185. <https://doi.org/10.1016/j.pocean.2018.01.003>
- 1335 Sakka Hlaili, A., Grami, B., Niquil, N., Gosselin, M., Hamel, D., Troussellier, M., Hadj  
1336 Mabrouk, H., 2008. The planktonic food web of the Bizerte lagoon (south-western  
1337 Mediterranean) during summer: I. Spatial distribution under different anthropogenic  
1338 pressures. Estuarine, Coastal and Shelf Science 78, 61–77.  
1339 <https://doi.org/10.1016/j.ecss.2007.11.010>
- 1340 Sakka Hlaili, A.S., Niquil, N., Legendre, L., 2014. Planktonic food webs revisited: Reanalysis  
1341 of results from the linear inverse approach. Progress in Oceanography 120, 216–229.  
1342 <https://doi.org/10.1016/j.pocean.2013.09.003>
- 1343 Schückel, U., Nogues, Q., Brito, J., Niquil, N., Blomqvist, M., Sköld, M., Hansen, J., Jakobsen,  
1344 H. and Morato, T. 2022. Pilot Assessment of Ecological Network Analysis Indices. In:  
1345 OSPAR, 2023: The 2023 Quality Status Report for the North-East Atlantic. OSPAR  
1346 Commission, London.
- 1347 Sharp, J.H., Peltzer, E.T., Alperin, M.J., Cauwet, G., Farrington, J.W., Fry, B., Karl, D.M.,  
1348 Martin, J.H., Spitzzy, A., Tugrul, S., Carlson, C.A., 1993. Procedures subgroup report.  
1349 Marine Chemistry, Measurement of Dissolved Organic Carbon and Nitrogen in Natural  
1350 Waters 41, 37–49. [https://doi.org/10.1016/0304-4203\(93\)90104-V](https://doi.org/10.1016/0304-4203(93)90104-V)
- 1351 Sherr, E.B., Sherr, B.F., 1993. Preservation and Storage of Samples for Enumeration of  
1352 Heterotrophic Protists, in: Handbook of Methods in Aquatic Microbial Ecology. CRC  
1353 Press.
- 1354 Sintes, E., Martínez-Taberner, A., Moyà, G., Ramon, G., 2004. Dissecting the microbial food  
1355 web: structure and function in the absence of autotrophs. Aquatic Microbial Ecology  
1356 37, 283–293. <https://doi.org/10.3354/ame037283>
- 1357 Siokou-Frangou, I., Christaki, U., Mazzocchi, M.G., Montresor, M., Ribera d’Alcalá, M.,  
1358 Vaqué, D., Zingone, A., 2010. Plankton in the open Mediterranean Sea: a review.  
1359 Biogeosciences 7, 1543–1586. <https://doi.org/10.5194/bg-7-1543-2010>
- 1360 Sreekanth, G.B., Chakraborty, S.K., Jaiswar, A.K., Zacharia, P.U., Mohamed, K.S., 2021.  
1361 Modeling the impacts of fishing regulations in a tropical Indian estuary using Ecopath  
1362 with Ecosim approach. Environ Dev Sustain 23, 17745–17763.  
1363 <https://doi.org/10.1007/s10668-021-01410-3>
- 1364 Steenbeek, J., Corrales, X., Platts, M., Coll, M., 2018. Ecosampler: A new approach to assessing  
1365 parameter uncertainty in Ecopath with Ecosim. SoftwareX 7, 198–204.  
1366 <https://doi.org/10.1016/j.softx.2018.06.004>
- 1367 Steinberg, D.K., Carlson, C.A., Bates, N.R., Goldthwait, S.A., Madin, L.P., Michaels, A.F.,  
1368 2000. Zooplankton vertical migration and the active transport of dissolved organic and  
1369 inorganic carbon in the Sargasso Sea. Deep Sea Research Part I: Oceanographic  
1370 Research Papers 47, 137–158. [https://doi.org/10.1016/S0967-0637\(99\)00052-7](https://doi.org/10.1016/S0967-0637(99)00052-7)
- 1371 Subramaniam, R.C., Corney, S.P., Melbourne-Thomas, J., Péron, C., Ziegler, P., Swadling,  
1372 K.M., 2022. Spatially explicit food web modelling to consider fisheries impacts and  
1373 ecosystem representation within Marine Protected Areas on the Kerguelen Plateau.  
1374 ICES Journal of Marine Science 79, 1327–1339.  
1375 <https://doi.org/10.1093/icesjms/fsac056>
- 1376 Taffi, M., Paoletti, N., Liò, P., Pucciarelli, S., Marini, M., 2015. Bioaccumulation modelling  
1377 and sensitivity analysis for discovering key players in contaminated food webs: The  
1378 case study of PCBs in the Adriatic Sea. Ecological Modelling, Special Issue: Ecological  
1379 Modelling for Ecosystem Sustainability: Selected papers presented at the 19th ISEM  
1380 Conference, 28-31 October 2013, Toulouse, France 306, 205–215.  
1381 <https://doi.org/10.1016/j.ecolmodel.2014.11.030>
- 1382 Tecchio, S., Chaalali, A., Raoux, A., Tous Rius, A., Lequesne, J., Girardin, V., Lassalle, G.,  
1383 Cachera, M., Riou, P., Lobry, J., Dauvin, J.-C., Niquil, N., 2016. Evaluating ecosystem-  
1384 level anthropogenic impacts in a stressed transitional environment: The case of the

- 1385 Seine estuary. *Ecological Indicators* 61, 833–845.  
1386 <https://doi.org/10.1016/j.ecolind.2015.10.036>
- 1387 Tecchio, S., Rius, A.T., Dauvin, J.-C., Lobry, J., Lassalle, G., Morin, J., Bacq, N., Cachera, M.,  
1388 Chaalali, A., Villanueva, M.C., Niquil, N., 2015. The mosaic of habitats of the Seine  
1389 estuary: Insights from food-web modelling and network analysis. *Ecological Modelling*  
1390 312, 91–101. <https://doi.org/10.1016/j.ecolmodel.2015.05.026>
- 1391 Templado, J., 2014. Future Trends of Mediterranean Biodiversity, in: Goffredo, S., Dubinsky,  
1392 Z. (Eds.), *The Mediterranean Sea*. Springer Netherlands, Dordrecht, pp. 479–498.  
1393 [https://doi.org/10.1007/978-94-007-6704-1\\_28](https://doi.org/10.1007/978-94-007-6704-1_28)
- 1394 Thomas, C.R., Christian, R.R., 2001. Comparison of nitrogen cycling in salt marsh zones  
1395 related to sea-level rise. *Marine Ecology Progress Series* 221, 1–16.  
1396 <https://doi.org/10.3354/meps221001>
- 1397 Tseng, L.-C., Kumar, R., Dahms, H.-U., Chen, Q.-C., Hwang, J.-S., 2008. Copepod Gut  
1398 Contents, Ingestion Rates, and Feeding Impacts in Relation to Their Size Structure in  
1399 the Southeastern Taiwan Strait. *Zoological Studies* 15.
- 1400 Turner, R.E., 2002. Element ratios and aquatic food webs. *Estuaries* 25, 694–703.  
1401 <https://doi.org/10.1007/BF02804900>
- 1402 Ulanowicz, R., 1997. *Ecology, the Ascendent Perspective*. Columbia University Press, New  
1403 York.
- 1404 Ulanowicz, R., 1992. Ecosystem health and trophic flow networks. pp. 190–225.
- 1405 Ulanowicz, R., 1986. PHENOMENOLOGICAL PERSPECTIVE OF ECOLOGICAL  
1406 DEVELOPMENT. ASTM Special Technical Publication 73–81.
- 1407 Ulanowicz, R.E., 2004. Quantitative methods for ecological network analysis. *Computational*  
1408 *Biology and Chemistry* 28, 321–339.  
1409 <https://doi.org/10.1016/j.combiolchem.2004.09.001>
- 1410 Ulanowicz, R.E., Goerner, S.J., Lietaer, B., Gomez, R., 2009. Quantifying sustainability:  
1411 Resilience, efficiency and the return of information theory. *Ecological Complexity* 6,  
1412 27–36. <https://doi.org/10.1016/j.ecocom.2008.10.005>
- 1413 Utermöhl, H., 1931. Neue Wege in der quantitativen Erfassung des Plankton.(Mit besonderer  
1414 Berücksichtigung des Ultraplanktons.). *SIL Proceedings, 1922-2010* 5, 567–596.  
1415 <https://doi.org/10.1080/03680770.1931.11898492>
- 1416 Vargas, C.A., González, H.E., 2004. Plankton community structure and carbon cycling in a  
1417 coastal upwelling system. II. Microheterotrophic pathway. *Aquatic Microbial Ecology*  
1418 34, 165–180. <https://doi.org/10.3354/ame034165>
- 1419 Vargha, A., Delaney, H.D., 2000. A Critique and Improvement of the CL Common Language  
1420 Effect Size Statistics of McGraw and Wong. *Journal of Educational and Behavioral*  
1421 *Statistics* 25, 101–132. <https://doi.org/10.3102/10769986025002101>
- 1422 Vasconcellos, M., Mackinson, S., Sloman, K., Pauly, D., 1997. The stability of trophic mass-  
1423 balance models of marine ecosystems: a comparative analysis. *Ecological Modelling*  
1424 100, 125–134. [https://doi.org/10.1016/S0304-3800\(97\)00150-6](https://doi.org/10.1016/S0304-3800(97)00150-6)
- 1425 Vézina, A., Piatt, T., 1988. Food web dynamics in the ocean. I. Best-estimates of flow networks  
1426 using inverse methods. *Mar. Ecol. Prog. Ser.* 42, 269–287.  
1427 <https://doi.org/10.3354/meps042269>
- 1428 Vézina, A.F., Pahlow, M., 2003. Reconstruction of ecosystem flows using inverse methods:  
1429 how well do they work? *Journal of Marine Systems, The Use of Data Assimilation in*  
1430 *Coupled Hydrodynamic, Ecological and Bio-geo-chemical Models of the Ocean.*  
1431 Selected papers from the 33rd International Liege Colloquium on Ocean Dynamics,  
1432 held in Liege, Belgium on May 7-11th, 2001. 40–41, 55–77.  
1433 [https://doi.org/10.1016/S0924-7963\(03\)00013-7](https://doi.org/10.1016/S0924-7963(03)00013-7)
- 1434